PLOS COMPUTATIONAL BIOLOGY

RESEARCH ARTICLE

Modeling spatial evolution of multi-drug resistance under drug environmental gradients

Tomas Ferreira Amaro Freire[1], Zhijian Hu[2], Kevin B. Wood[2], Erida Gjini[1]*

1 Center for Computational and Stochastic Mathematics, Instituto Superior Técnico, University of Lisbon, Lisbon, Portugal, **2** Departments of Biophysics and Physics, University of Michigan, United States of America

* erida.gjini@tecnico.ulisboa.pt

OPEN ACCESS

Citation: Freire TFA, Hu Z, Wood KB, Gjini E (2024) Modeling spatial evolution of multi-drug resistance under drug environmental gradients. PLoS Comput Biol 20(5): e1012098. https://doi.org/10.1371/journal.pcbi.1012098

Editor: Roger Dimitri Kouyos, University of Zurich, SWITZERLAND

Received: November 17, 2023

Accepted: April 23, 2024

Published: May 31, 2024

Data Availability Statement: All the data and codes are included in the manuscript and its supplementary materials.

Funding: TFAF was partly supported by grant GL Proj.2022/0006 awarded by Fundação Luso-Americana para o Desenvolvimento (FLAD). EG acknowledges support by the Portuguese Foundation for Science and Technology, FCT (CEECIND/03051/2018, 10.54499/2022.03060.PTDC and UIDB/04621/2020). KBW is supported by NIH R35GM124875. The funders had no role in

Abstract

Multi-drug combinations to treat bacterial populations are at the forefront of approaches for infection control and prevention of antibiotic resistance. Although the evolution of antibiotic resistance has been theoretically studied with mathematical population dynamics models, extensions to spatial dynamics remain rare in the literature, including in particular spatial evolution of multi-drug resistance. In this study, we propose a reaction-diffusion system that describes the multi-drug evolution of bacteria based on a drug-concentration rescaling approach. We show how the resistance to drugs in space, and the consequent adaptation of growth rate, is governed by a Price equation with diffusion, integrating features of drug interactions and collateral resistances or sensitivities to the drugs. We study spatial versions of the model where the distribution of drugs is homogeneous across space, and where the drugs vary environmentally in a piecewise-constant, linear and nonlinear manner. Although in many evolution models, per capita growth rate is a natural surrogate for fitness, in spatially-extended, potentially heterogeneous habitats, fitness is an emergent property that potentially reflects additional complexities, from boundary conditions to the specific spatial variation of growth rates. Applying concepts from perturbation theory and reaction-diffusion equations, we propose an analytical metric for characterization of *average mutant fitness* in the spatial system based on the principal eigenvalue of our linear problem, λ_1. This enables an accurate translation from drug spatial gradients and mutant antibiotic susceptibility traits to the relative advantage of each mutant across the environment. Our approach allows one to predict the precise outcomes of selection among mutants over space, ultimately from comparing their λ_1 values, which encode a critical interplay between growth functions, movement traits, habitat size and boundary conditions. Such mathematical understanding opens new avenues for multi-drug therapeutic optimization.

Author summary

In this study we develop a framework to model multi-drug resistance evolution in space by combining drug-rescaling arguments with a reaction-diffusion type model. In response

study design, data collection and analysis, decision to publish, or preparation of the manuscript.

Competing interests: The authors have declared that no competing interests exist.

to multi-drug environmental gradients, each independent mutant can grow and diffuse following an individual spatially-varying growth function and diffusion rate. Applying concepts from perturbation theory and reaction-diffusion models, we propose an analytical metric to quantify average mutant fitness in the spatial system and to predict the outcome of selection. Our findings highlight that in spatially-extended habitats fitness is an emergent property that potentially integrates many complexities, from boundary conditions to environmental variation, as well as individual growth and diffusion traits.

Introduction

Bacterial resistance to antibiotics remains one of the biggest threats to public health. The emergence and selection of strains that are resistant to multiple antibiotics exacerbates the problem of resistance management and control [1–4]. Different strategies have been proposed to mitigate the problem of antibiotic resistance, including antibiotic cycling vs. mixing patterns [5–9], synergies with the host immune defenses [10], maintenance of competition with sensitive strains [11–14], and–crucially–multidrug evolutionary strategies [15]. Although the molecular mechanisms underlying the rapid evolution of drug resistance are increasingly understood, it remains difficult to link this molecular and genetic information with multi-species population dynamics at different scales [16–19]. In addition, while the majority of studies focus on bacteria populations in well-mixed environments [20–22], natural communities evolve on spatially extended habitats that display multiple biotic and abiotic gradients [23, 24] and potentially yield complicated networks of interacting subpopulations [25, 26].

Understanding the role of this spatial structure in the evolution of resistance is an ongoing challenge, despite the fact that environmental drivers of evolution–for example, the local concentration of antibiotic, or the density of susceptible hosts–are known to vary on multiple scales–across different body compartments, organs, or tissues, and on longer length scales, between hospitals and geographic regions.

The impact of spatial heterogeneity on ecological and evolutionary dynamics has been studied in a wide range of contexts–from the spread of SARS-Cov2 [27] and HIV [28, 29] to conservation ecology [30, 31]. Graph theory and dynamical systems theory offer a number of elegant approaches for studying multi-habitat models on networks [32, 33] or in particular limits (e.g. with a center manifold reduction) [34]. Theory indicates that the way different subpopulations in a community are topologically "connected" can alter evolution [33, 35], and laboratory experiments in microbes are beginning to confirm some of these predictions [36, 37]. In parallel, a separate body of work has focused on spatial dynamics of microbial communities on agar plates, leading to an increasingly mature understanding of range expansions and cooperation in multi-species communities [38–43] or in populations impacted by complex fluid dynamics [44, 45].

In the specific context of drug resistance, spatial heterogeneity can manifest in multiple ways, from heterogeneity in drug concentrations to host heterogeneity in infectious disease models [46–49]. A number of theoretical and experimental studies have shown that spatial differences in drug concentration significantly impact the evolution of resistance [15, 50–59]. Theory suggests that the presence of spatial gradients of drug tends to accelerate resistance evolution [52, 54–56, 58], though it can be slowed down by tuning the drug profiles [60] or in cases where the fitness landscape is non-monotonic [53].

The connection between spatial heterogeneity and the evolution of resistance is particularly murky when multiple drugs are involved, making predictions difficult, both at a within-host

level in a clinical setting, as well as at the higher population or ecological levels [61, 62]. Even in the absence of spatial structure, multi-drug therapies are a subject of intense interest. Antibiotics interact when the combined effect of the drugs is greater than (synergy) or less than (antagonism) expected based on the effects of the drugs alone [63, 64], and these interactions can accelerate, reduce, or even reverse the evolution of resistance [65–70]. In addition to these interactions, which occur when drugs are used simultaneously, resistance to different drugs is linked through collateral effects–where resistance to one drug is associated with modulated resistance to other drugs. Collateral effects have been recently shown to significantly modulate resistance evolution [71–77].

Despite substantial progress in understanding spatial heterogeneity, drug interactions, and collateral effects separately, it remains unclear how these three components combine to impact the evolution of multi-drug antibiotic resistance. To address this gap, we study a general mathematical model describing a continuous environment with spatially-varying antibiotic concentrations, in which bacteria move, grow and are selected following deterministic dynamics. Our aim is to build an integrative framework for drug interactions and collateral effects in spatially-extended multi-drug environments and show how specific drug gradients can shape evolutionary outcomes.

The outline of the paper is as follows. In Section 2 we present the spatial model, extending the model–first introduced in [70] for multi-drug resistance evolution (summarized in Box 1). In Section 3, we present an analytical quantity for predicting outcomes of selection in multi-drug spatial environments, and describe key cases of multi-drug resistance evolution linking simulations with theoretical predictions. We conclude with a discussion of our study's limitations and potential future extensions.

Materials and methods

The model extended to space and spatial gradients of 2 drugs

We consider the case of a population of bacteria growing and randomly diffusing in space (1-d) as a finite set of M subpopulations (mutants/strains), where each mutant has a potentially different level of resistance to the drugs (Box 1). The total population size at each point in space (z) is given by $n(z,t) = \sum_{i=1}^{M} n_i(z,t)$, with the dynamics of the subpopulations given by

$$\frac{\partial n_i(z,t)}{\partial t} = g_i n_i + D\frac{\partial^2 n_i}{\partial z^2} \tag{6}$$

where D represents the common diffusion coefficient, g_i the growth rate of mutant i. For simplicity we choose

$$\begin{aligned} n_i(0,t) &= n_i(L,t) = 0 \\ n_i(z,0) &= n_{0,i}(z) \end{aligned} \tag{7}$$

where $n_{0,i}$ the initial distribution of mutant i. This system is an instance of the classical reaction-diffusion system with exponential growth kinetics, and Dirichlet boundary conditions. The assumption is that bacteria live in an idealized one-dimensional fixed domain of length L, and die when moving out the habitat, either because they meet inhospitable conditions or because of lack of resources for growth. Within the domain, we assume there are unlimited resources for growth, and there is no direct interaction between the mutants i.e. all of them are assumed to grow exponentially independently of each other. These assumptions would naturally apply in situations where population density is far below carrying capacity, yet these models may guide intuition even beyond these strict limits. For example, recent work investigating

Box 1. Modeling framework for multidrug resistance

Drug resistance as a rescaling of effective drug concentration

To link a cell's level of antibiotic resistance with its fitness in a given multidrug environment, we assume that drug-resistant mutants exhibit phenotypes identical to those of the ancestral ("wild type") cells but at rescaled effective drug concentration [65, 70]. The phenotypic response (e.g. growth rate) of drug-resistant mutants corresponds to a rescaling of the growth rate function $G(x, y)$, of the ancestral population at concentrations x and y of the two drugs. At such concentrations, the per-capita growth rate (g_i) of mutant i is given by

$$g_i = G(\alpha_i x, \beta_i y), \tag{1}$$

where α_i and β_i are rescaling parameters that reflect an effective change in drug concentration and, therefore, in mutant's subpopulation growth rate.

Mutant traits

In a 2-drug environment, each mutant i is characterized by a pair of scaling parameters,

$$(\alpha_i, \beta_i) = (\text{susceptibility to drug 1, susceptibility to drug 2}), \tag{2}$$

which one might think of as a type of coarse-grained genotype. When $0 < \alpha, \beta < 1$, the mutant has partial susceptibility to each drug. When either is equal to 0 or 1, this reflects full resistance or susceptibility to that drug. The reference WT in this rescaling has trait (1, 1). The rescaling factors can be measured experimentally, for example, as the ratios of the mutant MICs for two different antibiotics relative to those of the wild-type.

Mean trait evolution and population adaptation

Considering all growth rates g_i of existing mutants (e.g. $i = 1, ..M$), the population dynamics of scaling parameters follows naturally as a dynamic weighted average over all sub-populations. The mean resistance traits to drugs 1 and 2, (averaged over all mutants) $\bar{\alpha}(t) \equiv \sum_{i=1}^{M} \alpha_i f_i(t)$, and $\bar{\beta}(t)$ evolve as:

$$\frac{d\bar{\alpha}}{dt} = \sum_{i=1}^{M} \alpha_i \frac{df_i(t)}{dt}, \qquad \frac{d\bar{\beta}}{dt} = \sum_{i=1}^{M} \beta_i \frac{df_i(t)}{dt}, \tag{3}$$

where $f_i(t)$ is the frequency of mutant i at time t in the population. Assuming exponential growth ($dn_i/dt = g_i n_i$), with n_i the abundance of mutant i and g_i given by Eq 1, the frequency $f_i(t)$ changes according to a replicator equation [78]:

$$\frac{df_i}{dt} = \frac{d}{dt}\left(\frac{n_i}{\sum_i n_i}\right) = f_i(g_i - \bar{g}), \tag{4}$$

where $\bar{g} = \sum_{i=1}^{M} f_i g_i$ is the (time-dependent) mean value of g_i across all M subpopulations. In our case, i.e. under no interactions, g_i is an exponential, frequency-independent, mutant growth rate.

The Price equation for mean trait evolution

Combining equations, we arrive at:

$$\frac{d\bar{\alpha}}{dt} = \mathrm{Cov}_{\boldsymbol{x}}(\alpha, g), \qquad \frac{d\bar{\beta}}{dt} = \mathrm{Cov}_{\boldsymbol{x}}(\beta, g). \tag{5}$$

where $\mathrm{Cov}(\alpha, g)_{\boldsymbol{x}} \equiv \sum_{i=1}^{M} \alpha_i f_i (g_i - \bar{g})$ is the covariance between the scaling parameters α_i and the corresponding mutant growth rates g_i, and similarly for $\mathrm{Cov}(\beta, g)_{\boldsymbol{x}}$. The subscript $\boldsymbol{x}$ refers to the fact that the growth rates g_i and $\bar{g}$ depend on the external (true) drug concentration $\boldsymbol{x} \equiv (x, y)$.

drug holidays in cancer showed that simple exponential growth models offer accurate predictions of optimal drug regimens in laboratory experiments and simulated tumors with substantial spatial structure and competition [79].

Linking the model to multi-drug resistance: $g_i = G(\alpha_i x, \beta_i y)$

While the system 6 can be studied on its own, just as an abstract framework for mutants which vary in their growth rates and diffuse over space, here we focus on the key scenario that growth rate is entirely determined by the (α_i, β_i) antibiotic resistance trait of each mutant and the two drug concentrations (x, y) (see Box 1). Specifically we consider two cases:

- Case 1: $g_i = G(\alpha_i x, \beta_i y)$ is constant in space, i.e. a spatially *homogeneous* 2-drug environment (concentrations of both drugs are constant over space). This leads to a constant selection coefficient everywhere in space. The frequency equation for each mutant in this case is given by the PDE:

$$\frac{\partial f_i(z,t)}{\partial t} = f_i(g_i - \bar{g}) + D\frac{\partial^2 f_i}{\partial z^2}, \tag{8}$$

  related to the Fisher-KPP equation [80, 81]. For example for 2 mutants with $g_1 > g_2$, Eq 8 is equivalent to $\frac{\partial f_1}{\partial t} = (g_1 - g_2) f_1 (1 - f_1) + D\frac{\partial^2 f_1}{\partial z^2}$, describing the classical Fisher equation with logistic growth and simple Fickian diffusion.

- Case 2: $g_i(z) = G(\alpha_i x(z), \beta_i y(z))$ varies in space, i.e. a spatially *inhomogeneous* 2-drug environment, with drug concentrations that vary in z. This leads to a selection coefficient among mutants that is space-dependent, hence the frequency of each mutant at each point in space changes according to:

$$\frac{\partial f_i(z,t)}{\partial t} = f_i(g_i(z) - \bar{g}(z,t)) + D\frac{\partial^2 f_i}{\partial z^2}, \tag{9}$$

  where $\bar{g}(z,t) = \sum_i f_i(z,t) g_i(z)$.

Initially we assume equal movement traits between all mutants, translating into equal diffusivities D, hence only growth differences driving a fitness gradient. The function G can be constructed analytically using abstract functional forms for antagonistic, synergistic or independent drug action [63], or can be obtained empirically from growth measurement of

wild-type bacteria (or an arbitrary reference strain) at a range of two-drug combination doses $(x, y) \in [x_{min}, x_{max}] \times [y_{min}, y_{max}]$. (see, for example, [69]).

In what follows, we investigate 3 broad regimes for G, corresponding to i) independent drug action, ii) synergistic drug interaction, iii) antagonistic drug interaction. From Eq 9 we can expect that a mutant will grow in frequency at some point in space only if its growth rate is higher than the population's mean growth at that point in space but diffusion can play a role in transiently reverting this trend and determining the final outcome.

Multi-drug resistance evolution in space. Combining equations above, we arrive at the following PDE system governing evolution of mean rescaling factors to drug 1 ($\bar{\alpha}$), and drug 2 ($\bar{\beta}$), a measure of multi-drug resistance:

$$\frac{\partial \bar{\alpha}}{\partial t} = Cov_x(\alpha, g) + D\frac{\partial^2 \bar{\alpha}}{\partial z^2},$$

$$\frac{\partial \bar{\beta}}{\partial t} = Cov_x(\beta, g) + D\frac{\partial^2 \bar{\beta}}{\partial z^2}.$$

This is a Price equation [82, 83] in space, different from the non-spatial Price equation derived in our earlier study [70]. This equation highlights how the evolution of mean traits depends on their covariance with growth rate at each point in time and space. However compared to the non-spatial model (Box 1), in this case we are dealing with two partial differential equations, because the mean traits $\bar{\alpha}(z, t)$ and $\bar{\beta}(z, t)$ now evolve over space and time.

Numerical prediction of selection dynamics. While the Price Equation framework is compact, it is not by itself sufficient to predict evolution over multiple time steps since the covariance terms are dynamic. We need the explicit mutant frequencies information at a given time-point to be able to simulate the system. Thus, provided with initial conditions, i.e. an initial spatial distribution over space for all mutants, and their multi-drug resistance traits (α_i, β_i), given a drug-action landscape G and an external drug concentration $(x(z), y(z))$ we can numerically integrate the equations to obtain solutions $f_i(z, t)$ for frequencies of all mutants, and finally $\bar{\alpha}(z, t)$ and $\bar{\beta}(z, t)$ as well as mean adaptation rate of the population $\bar{g}(z, t) = \sum_i f_i(z, t) g_i(z)$.

Results

In this study, we consider the context of a cellular population adapting to a multi-drug environment via selection of pre-existing diversity. Although another route to adaptation is provided by *de-novo* mutations, we limit ourselves here to the case of standing variation, where antibiotic-resistant mutants with different degrees of susceptibility to two drugs are already present from the start, albeit at possibly very low frequencies. We investigate if and how a spatial pattern of diversity in antibiotic resistance phenotypes distribution over long time scales emerges from the fitness gradient between such mutants. We observe that a variety of selection outcomes are possible in such growing population. We distinguish two qualitative regimes for spatial heterogeneity: i) constant drug concentration over space, and ii) spatially-varying drug concentrations, leading to constant and spatially-varying mutant growth rates over space respectively.

The main novelty of our approach is that beyond numerical simulations of the model PDEs, we propose a fully analytical measure of mutant fitness over space via which the outcome of selection can be predicted, studied and controlled.

An average fitness measure to predict selection outcome

When the mutants have the same growth rate everywhere in space, it is intuitive to compare them via their Fisher speed of propagation $c = 2\sqrt{Dg_i}$, hence by their growth rates. Yet, when the growth rate is a space-dependent function, it is not clear how to establish fitness hierarchies. Our system is governed by the PDE

$$\frac{\partial n}{\partial t} = g(z)n + D\frac{\partial^2 n}{\partial z^2}, \quad z \in [0, L] \tag{10}$$

which describes each sub-population. Assuming separation of variables, and rescaling space to [0, 1] we can arrive at the following eigenvalue equation (see S1):

$$\begin{aligned} \frac{\partial^2 u}{\partial z^2} + \left(\frac{g(zL)L^2}{D} - \lambda\right)u &= 0, \quad z \in [0, 1] \\ u(0) &= u(1) = 0 \end{aligned} \tag{11}$$

where u is the eigenfunction corresponding to eigenvalue λ. This falls within classical Sturm-Liouville problems, whose spectrum consists of a discrete set of eigenvalues λ_n (in our case, decreasing) that determine the behavior of solutions. Importantly, when the principal eigenvalue of the operator is positive, $\lambda_1 > 0$, it follows that the solutions grow away from zero, corresponding to the trivial spatially homogeneous steady state (no bacteria) being unstable. The fact that $\lambda_1 > 0$ ensures growth is shown in the S1 Text, Sections A-C. These eigenvalues can be numerically computed and evaluated but they can also be analytically bounded using variational methods, or analytically approximated. The latter is the approach we adopt here.

By assuming that $g(z)$ can be written as $g_{max}g_0(z)$ such that $\epsilon \equiv g_{max}L^2/D \ll 1$ is a small parameter that describes the ratio of the two relevant timescales: the timescale for diffusion (L^2/D) and that for growth ($1/g_{max}$, with g_{max} a suitable scaling factor, e.g. the maximum value of $g(z)$), the eigenvalue equation above becomes:

$$\frac{\partial^2 u}{\partial z^2} + \epsilon g_0(zL)u = \lambda u, \tag{12}$$

For small $\epsilon \ll 1$, it is straightforward to derive expressions for λ via classical perturbation theory (see S1 Text A-C), leading to an expression for the nth eigenvalue λ_n, up to any order in ϵ. In particular for first-order approximation we obtain:

$$\lambda_n = -n^2\pi^2 + 2\epsilon\int_0^1 g_0(zL)\sin^2(n\pi z)dz, \quad z \in [0, 1]. \tag{13}$$

In the above expression, we can substitute ϵ explicitly. Then, reverting to original space and for $n = 1$, we obtain the following principal eigenvalue approximation:

$$\lambda_1 \approx -\frac{\pi^2 D}{L^2} + \frac{2}{L}\int_0^L g(z)\sin^2\left(\frac{\pi z}{L}\right)dz \quad z \in [0, L] \tag{14}$$

This principal eigenvalue, in the case of a single population, holds key information for successful invasion, and in the case of multiple mutants, can be used to determine their relative success in growth and propagation over space. It is noteworthy to remark that although strictly-speaking, our approximation for λ_1 is based on assuming $\epsilon \ll 1$ the practical use of this asymptotic approximation typically gives reasonable results outside of its strict range of applicability. So in many numerical examples we find that the λ_1 approximation predicts very well the

outcome of selection also for small diffusion rates. However, formally the other extreme of the perturbation approach (growth much faster than diffusion) is analyzed in S1 Text, Section B.

Special case: Constant $g(z) \equiv r$. In the case where growth rate is a constant r, Eq 14 for $n = 1$ yields the survival condition $\lambda_1 > 0$ which ultimately says that the growth rate $r > \frac{\pi^2 D}{L^2}$, a well known result from spatial spread models witht these boundary conditions [84], also framed as a critical length required for the trivial steady state to become unstable $L > L_c = \pi\sqrt{D/r}$ (see Eq S.23 in S1 Text). Following this reasoning, the magnitude of λ_1, can become a relative measure by which to compare also different mutants $i = 1, ..M$ growing and spreading in parallel. The mutant with the higher λ_1 should win. This condition can also be applied when mutants vary in their diffusion coefficients: the mutant with the smallest $\pi\sqrt{D_i/r_i}$ should exclude the others.

Arbitrary $g(z)$. In general, and when the population is comprised of more than one subpopulation each experiencing a different space-dependent growth rate $g_i(z)$, the largest eigenvalue (Eq 14) can be taken as a measure of average fitness over space for each mutant and we can expect that if we compare two mutants i and j, mutant i will ultimately dominate the population if $\lambda_1(i) > \lambda_1(j)$ and vice versa. For comparison with simulations, we also present a discrete-space analytical approximation for λ_1 and some key properties (Box 2).

Example dynamics in spatially homogeneous drug concentrations

For $g_i = G(\alpha_i x, \beta_i y)$, namely, when growth rates are independent of space, and assuming that different strains diffuse will equal rate D, the mutant with the highest positive g_i wins over long time everywhere in competitive exclusion. The spatial dynamics of the frequencies of each mutant correspond to a travelling wave, with speed of spread $c_i = 2\sqrt{Dg_i}$. When there is no variation in D, the mutant with the highest positive g_i tends to fixation everywhere, irrespective of how this g_i is determined by the confluence of resistance traits and 2-drug landscape in $G(\alpha_i x, \beta_i y)$, as illustrated in Fig 1. The only way for two (or more) mutants to coexist is when their fitnesses perfectly equalize, i.e. if their antibiotic resistance traits are such that g_i and g_j fall on the same contour of G: $G(\alpha_i x, \beta_i y) = G(\alpha_j x, \beta_j y)$. But the levels of such coexistence will depend on their initial total distribution, whereby the mutant with an overall advantage at the start, also persists at higher frequency in steady state coexistence.

Competitive exclusion when two mutants have constant g_i and g_j in $[0, L]$. Some examples of outcomes among two strains for constant g_i over space are illustrated in Fig 1. If these constant growth rates are different $g_i \neq g_j$, under equal initial conditions, the mutant with the higher g will spread faster and eventually take over everywhere in space (Fig 1A). In contrast, if these constant growth rates are equal, it is possible that asymmetric initial conditions create a bias and the mutant with a head start will eventually win (Fig 1B–1D). The bias can be created from total initial abundance (Fig 1C) or relative distribution over space (Fig 1D). In the latter case, the mutant with a relative advantage in the center of the domain will effectively spread faster and competitively exclude the other over all space.

Example dynamics under spatial gradients in drug concentrations

The case of $g_i(z) = G(\alpha_i x(z), \beta_i y(z))$, when the drug concentrations can vary over space, and hence also mutant selective advantages, is the more realistic, the more interesting and naturally the more complex one. We observe mainly two results: competitive exclusion with the same mutant winning everywhere or coexistence of the same subset of mutants everywhere (although at different frequencies). The final outcome depends on how average fitness over space compares between all mutants. Theoretically this PDE case is much more complex and

Box 2. How should we define global mutant fitness over space?

To go from spatial growth rate $g(z)$ variation among mutants to final selection outcome over space $z \in [0, L]$, we propose the use of the principal eigenvalue of the linearized equation for each mutant, λ_1. This should yield an exact measure of global fitness, which can be numerically computed or analytically approximated (see S1 Text, Section A) to obtain the mutant ranking.

λ_1 when space is discretized

We begin with some suitable discretization of space, for example by subdividing the interval $[0, L]$ with $K + 2$ equally spaced points (linearly-arranged patches with $h_z = \frac{L}{K+1}$). In the case where $\epsilon \equiv g_{max}L^2/D$ is relatively small, the λ Eq 14 for $n = 1$ can be approximated via second-order centered finite differences to represent the diffusion. Written in matrix form, where also the function $g(z)$ is now discretized as piecewise constant (g_k) within each small sub-interval k, we can then use a Taylor expansion to arrive at an approximation for the principal eigenvalue λ_1. The first-order approximation for λ_1, under mutant growth rate $g(z)$, for suitably high discrete resolution of space (K large) is given by:

$$\lambda_1 = -\frac{\pi^2 D}{L^2} + \frac{2}{K+1}\sum_{k=1}^{K} g_k \sin^2\left(\frac{k\pi L}{K+1}\right) \tag{15}$$

where k runs over all interior sub-intervals of space (See Section C in S1 Text).

Properties of λ_1 as a fitness measure over space

- Under Dirichlet boundary conditions, the λ_1 indicates that central parts of the domain have a higher value for growth than regions closer to the boundary. This can be seen from weighting of $g(z)$ via the function $\sin(z)^2$.
- Assuming that different strains have the same D, the between-mutant difference $\lambda_1(i) - \lambda_1(j)$ does not depend on diffusion (first-order approximation). Diffusion rate, D, when equal, cannot alter selection, but it can do so when it varies, i.e. $D_i \neq D_j$.
- In order to increase accuracy for growth functions that are very close, and enable selection sensitivity to a common diffusion rate, we must compute λ_1 by including additional higher-order terms in the Taylor approximation (see C.2 in S1 Text).
- The difference $\lambda_1(i) - \lambda_1(j)$, for equal D, will predict the same winner as the difference in spatially-averaged growth rates $\bar{g}_i - \bar{g}_j$ if $\Delta g(z) = g_i(z) - g_j(z)$ does not change sign over space z. This is key to compare selection under the spatial vs. non-spatial dynamics.
- Under equal diffusion rate D, through weighting of $\Delta g(z)$ via the function $\sin(z)^2$ inside the sum (Eq 15) and integral (Eq 14), it is evident that spatial growth function differences $\Delta g(z)$ which are symmetric around the center $(L/2)$, will yield $\lambda_1(i) = \lambda_1(j)$, hence coexistence between strains i and j, albeit under possible spatial segregation.

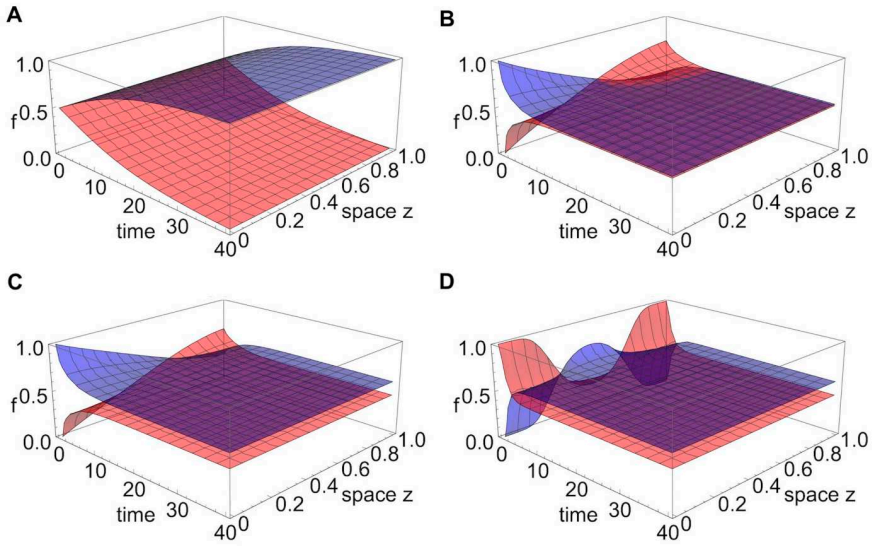

Fig 1. Example of outcomes among two strains for constant g_i over space. A. Competitive exclusion. In this example, strains start at uniform distribution over space, with $g_1 > g_2$, hence dynamics lead to a traveling wave solution for $f_1(z, t)$ and $f_2(z, t)$ with strain 1 traveling at faster speed and ultimately being the winner everywhere over long time. **B.** (Neutrally-stable) coexistence at 50:50 because the mutants start at equal total abundances and $g_1 = g_2$. **C.** (Neutrally-stable) coexistence different from 50:50 because mutants start at different total abundances and $g_1 = g_2$. **D.** (Neutrally-stable) coexistence different from 50:50 because mutants start at equal total abundances with $g_1 = g_2$, but their initial distribution over space favours one of them that starts at higher abundance in the center of the domain.

https://doi.org/10.1371/journal.pcbi.1012098.g001

analytical solutions have been obtained only for special cases under certain regularities. Below we consider some specific scenarios.

Coexistence under $g(z)$ variation but perfect (i, j) symmetry around $\frac{L}{2}$. An example of linear $g_i(z)$, $g_j(z)$ variation for 2 mutants leading to coexistence everywhere is shown in Fig 2. In this case, one strain is better-adapted in the first half of the domain, the other strain is better-adapted in the second-half of the domain with the selective advantages exactly counterbalanced (Fig 2A). For low diffusion, each strain dominates in frequency in the part of the domain where it experiences a relatively higher growth rate, maintaining a high-degree of spatial segregation in the system (Fig 2B). As diffusion increases, the coexistence frequencies become more similar and tend towards 1/2 in both halves of the domain, leading to a more homogeneous spatial distribution of the strains over space (Fig 2C and 2D).

Competitive exclusion under broken (i, j) symmetry around $\frac{L}{2}$, even with equal spatial averages of g. This is the example in Fig 3A, where $g_1(z)$ and $g_2(z)$ are piecewise-constant. For equal mean growth rates over space, the situation has been long tackled analytically [85, 86]. As recognized in previous theoretical studies, for Dirichlet boundary conditions, it is expected that the population with a spatial growth advantage in the center of the domain will experience the maximal fitness, and be the winner [85]. Indeed this is what we obtain when considering such piece-wise growth functions which make one mutant more suited to the center of the domain and the other mutant more suited to the borders of the domain. Even though mean growth rates are equal, the mutant with the central advantage spreads with an advantage and ultimately excludes the other everywhere in space.

In our case (Fig 3A), the spatial averages of the two mutant growth rates are simply $\bar{g_1} = L(bg_{max} + (1-b)g_{min})$ and $\bar{g_2} = L(bg_{min} + (1-b)g_{max})$, where g_{max}, g_{min} are the maximum

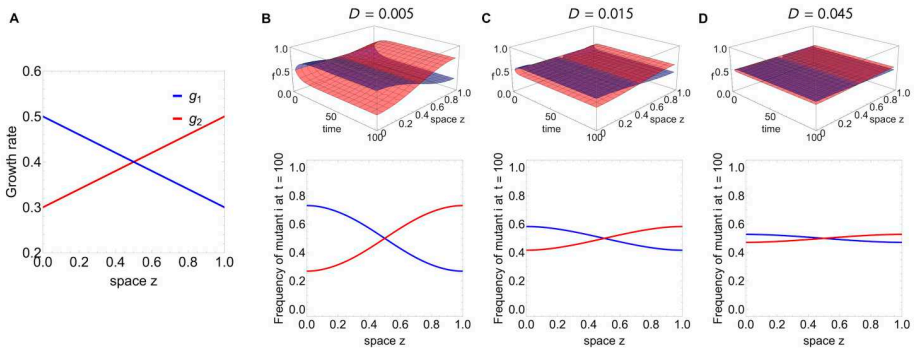

Fig 2. Coexistence example of 2 strains everywhere in space for space-dependent $g_i(z)$ which are mutually symmetric about $L/2$. A. In this case, one strain is better-adapted in the first half of the domain, the other strain is better-adapted in the second-half of the domain with the selective advantages exactly counterbalanced. **B.** For low diffusion, the two strains coexist such that each strain dominates in frequency in the part of the domain where it experiences a relatively higher growth rate, maintaining a high-degree of spatial segregation in the system. **C.** As diffusion increases, the coexistence frequencies become more similar and tend towards 1/2 in both halves of the domain. **D.** Eventually, for very high-diffusion, the growth variation starts to matter less and less, and the two strains tend to the same frequency everywhere, leading to a uniformly homogeneous spatial distribution of diversity over space.

https://doi.org/10.1371/journal.pcbi.1012098.g002

and minimum growth rate of each strain, and b the size of the centered region where $g_1 > g_2$. The condition for them to be equal for any g_{max} and g_{min} is simply $b = 1/2$. In concordance with previous theory, when $\bar{g_1} = \bar{g_2}$, we observe that the strain with the central advantage will be the ultimate winner in the system.

In contrast, the situation gets more complicated when spatially-averaged growth rates differ, hence $b \neq \frac{1}{2}$ such that $\bar{g_1} \neq \bar{g_2}$. It is not always the superiority in mean g or in central advantage that simply drives selection. We can find cases that the strain with central advantage in g (in this case strain 1) may lose overall because of its total growth rate, or when the strain with superior mean g may lose overall because of its central fitness disadvantage. The key lies in the relative λ_1 magnitude of each mutant.

Tuning spatial heterogeneity of g_i and g_j can invert selection. An example with nonlinear growth rates, leading to competitive exclusion with the possibility to revert the winner via a continuous parameter change is shown in Fig 3B. From the parabolic shapes of the growth rates it's not immediately clear which should be the strain to ultimately grow and spread faster over space. Using λ_1 calculations (Eq 14) for the difference between mutants, we find that for small values of the parameter h it is strain 2 that ultimately excludes strain 1, but for large enough h, more specifically

$$h > h_c = \frac{L^2(\pi^2 - 6)\sigma}{4\pi^2},$$

strain 1 overall fitness is superior and it will be this strain the only persisting one in the system. This result is impossible to disentangle from comparing purely spatial averages of the two growth rates. The information of the spatial average is insufficient because it weighs equally all points in space, whereas in reality the death at the boundary and the competition between diffusion and growth within the boundary makes locations near the centre of the domain be of higher value for any strain. The appropriate weighting of space is contained in the measure λ_1.

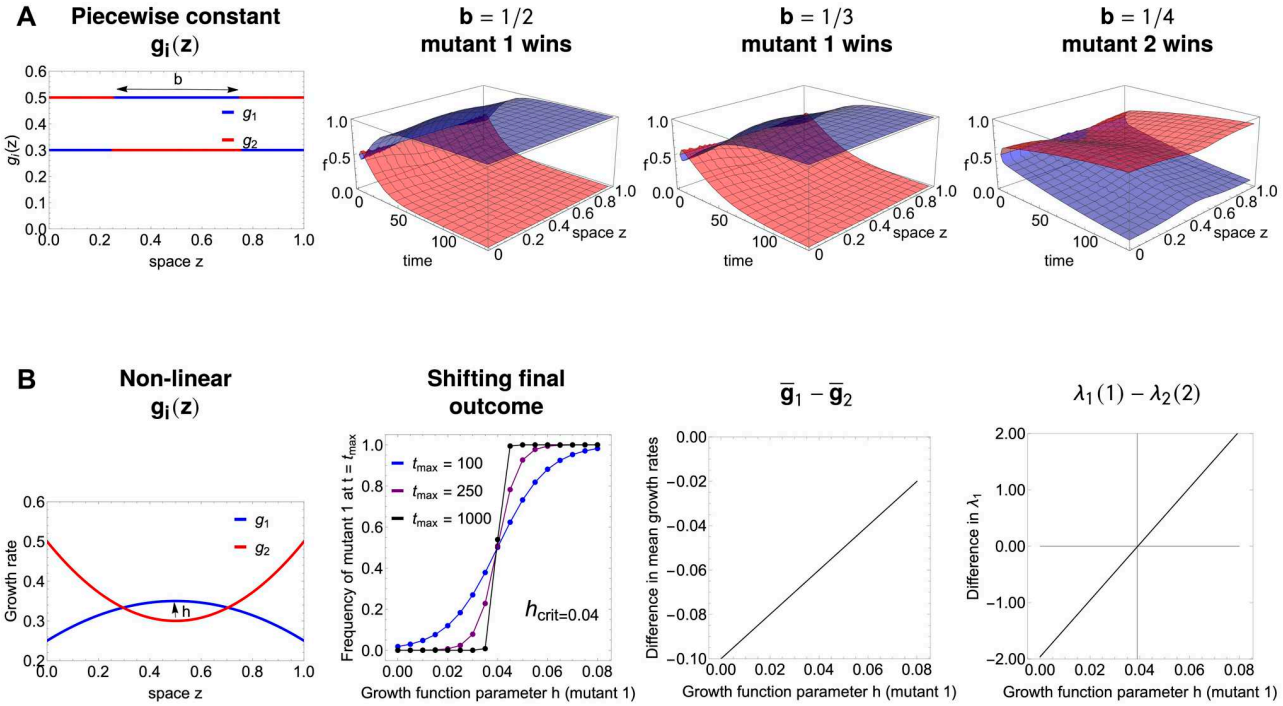

Fig 3. Competitive exclusion everywhere in space, but the ultimately winning strain depends on parameters of $g_i(z)$ variation. A. In this piece-wise growth rate example, the $g_1(z)$ and $g_2(z)$ are such that the mean growth rates for both strains are the same $\bar{g}_1 = \int_0^1 g_1(z)dz = \int_0^1 g_2(z)dz = \bar{g}_2$ for $b = 1/2$ and $g_{max} = 0.5$, $g_{min} = 0.3$. Yet, even with equal spatially-averaged growth rates, starting from equal initial distributions, the strain with the central advantage will be the winner. When b changes, the final winner is a result of b as well as $(max(g) - min(g))$ magnitude. **B.** In this example, the winner can be overturned by modulating the width of the interval where $g_1(z) > g_2(z)$, while keeping the shape of the two functions. We assume the growth rates are non-monotonic functions of space, represented by a concave and a convex parabola with vertices near the middle of the domain: $g_1(z) = m - \sigma(z - L/2)^2 + h$ and $g_2(z) = m + 2\sigma(z - L/2)^2$ with $m = 0.3$, $\sigma = 0.4$, $D = 0.015$ and h varied. The critical value of h for overturning the final outcome is $h = 0.04$. Mutant 1 loses if $h < 0.04$ but it wins if $h > 0.04$, when its fitness advantage in the center of the domain is sufficiently high to compensate for its disadvantage near the boundaries. This cannot be predicted with the mean growth rate difference $\bar{g}_1 - \bar{g}_2$ but can be predicted with λ_1 difference for mutants 1 and 2. See also S1 Mathematica Notebook.

https://doi.org/10.1371/journal.pcbi.1012098.g003

An 'atlas' of selection outcomes under drug spatial heterogeneity: Single or double resistance?

With this setup, it is now possible to systematically study scenarios of drug variation over space. First we focus just on 4 relevant mutants, which represent the main resistance combinations: mono-resistance to drug 1, and to drug 2, double intermediate resistance to both drugs, and wild-type (see Fig 4). These correspond to special locations in α, β space, namely (0, 1), (1, 0), (0.5, 0.5) and (1, 1). Then we consider synergistic vs. antagonistic drug interactions, under the assumption of a low diffusion rate, and several explicit 2-drug concentration variation patterns over space $x(z)$, $y(z)$. Although more complex fitness landscape formulations are possible [87], the growth rates we assume for the drug interaction as a function of drug concentrations x and y, can be constructed for illustration, via the following simple functions:

$$G(x,y) = \begin{cases} 2 - (x+y) - qxy, & \text{for synergistic drugs} \\ 2 - (x+y), & \text{for independent drugs} \\ 2 - (x+y) + qxy, & \text{for antagonistic drugs,} \end{cases} \quad (16)$$

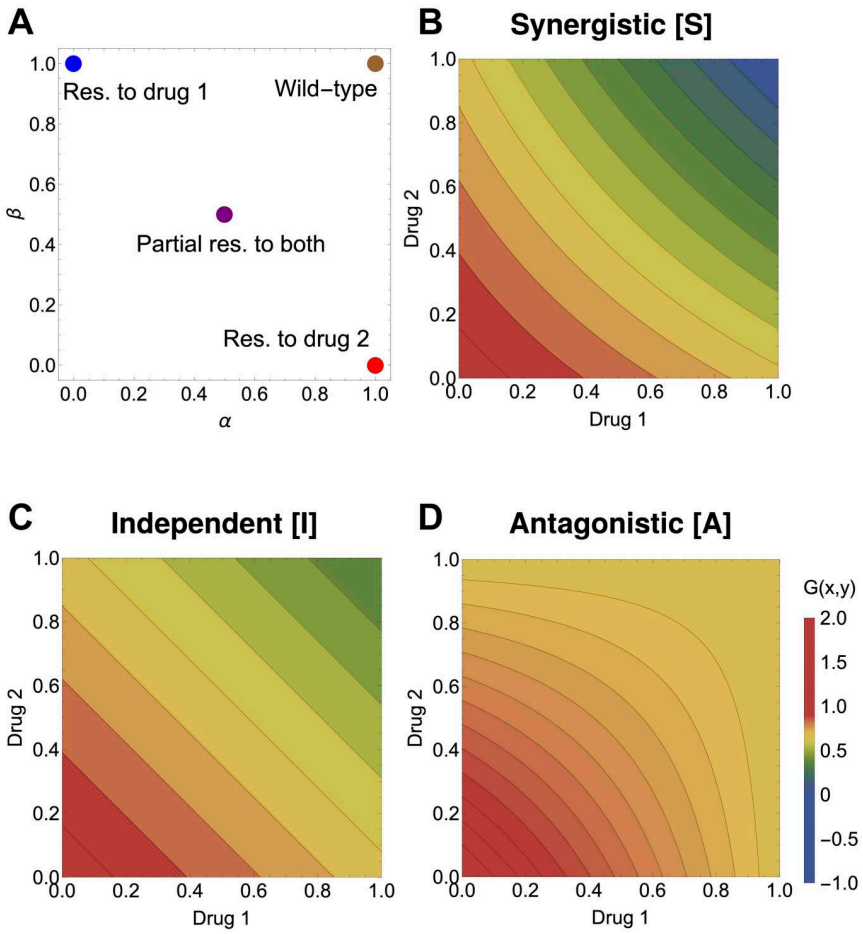

Fig 4. The basis for the atlas of multi-drug resistance evolution patterns over space. A. The four canonical mutant types for resistance phenotypes to two drugs, distributed in the (α, β) space of rescaling parameters: blue—fully resistant to drug 1 and sensitive to drug 2; red—fully resistant to drug 2 and sensitive to drug 1; purple—intermediate resistance to both drugs; brown—wild-type, sensitive to both drugs. The 3 drug fitness landscapes used are: **B.** synergistic, **C.** independent and **D.** antagonistic, as specified in Eq 16 for $q = 1$. These drug landscapes will be used to give rise to $g_i(z) = G(\alpha_i x(z), \beta_i y(z))$ as a function of two drug variation over space $x(z)$ and $y(z)$. The relative fitnesses of the strains are hence dependent both on drug variation over space and on the details of the underlying growth landscape G.

https://doi.org/10.1371/journal.pcbi.1012098.g004

where $q > 0$ and can be taken as a measure of the strength of interaction, illustrated in Fig 4B–4D, and G is symmetric with respect to each drug.

The results of simulations are presented in Fig 5. Different multidrug concentration gradients give rise to a total of 12 scenarios, a kind of 'atlas'. We show the frequencies obtained by simulating the system long enough for it to have reached a spatial equilibrium. These are not meant to be an exhaustive analysis but a summary of key cases of spatial heterogeneity that can shape evolution of multi-drug resistance along the main axes of monomorphic vs. polymorphic phenotypic distributions. A study of more multidrug scenarios, under a more complex growth function G, is shown in Supplementary Figs A-C in S1 Text, where we also explore different diffusion rates.

These scenarios show that exactly anti-symmetric drug gradients relative to the center of the spatial domain are those more likely to lead to coexistence of different types of resistances

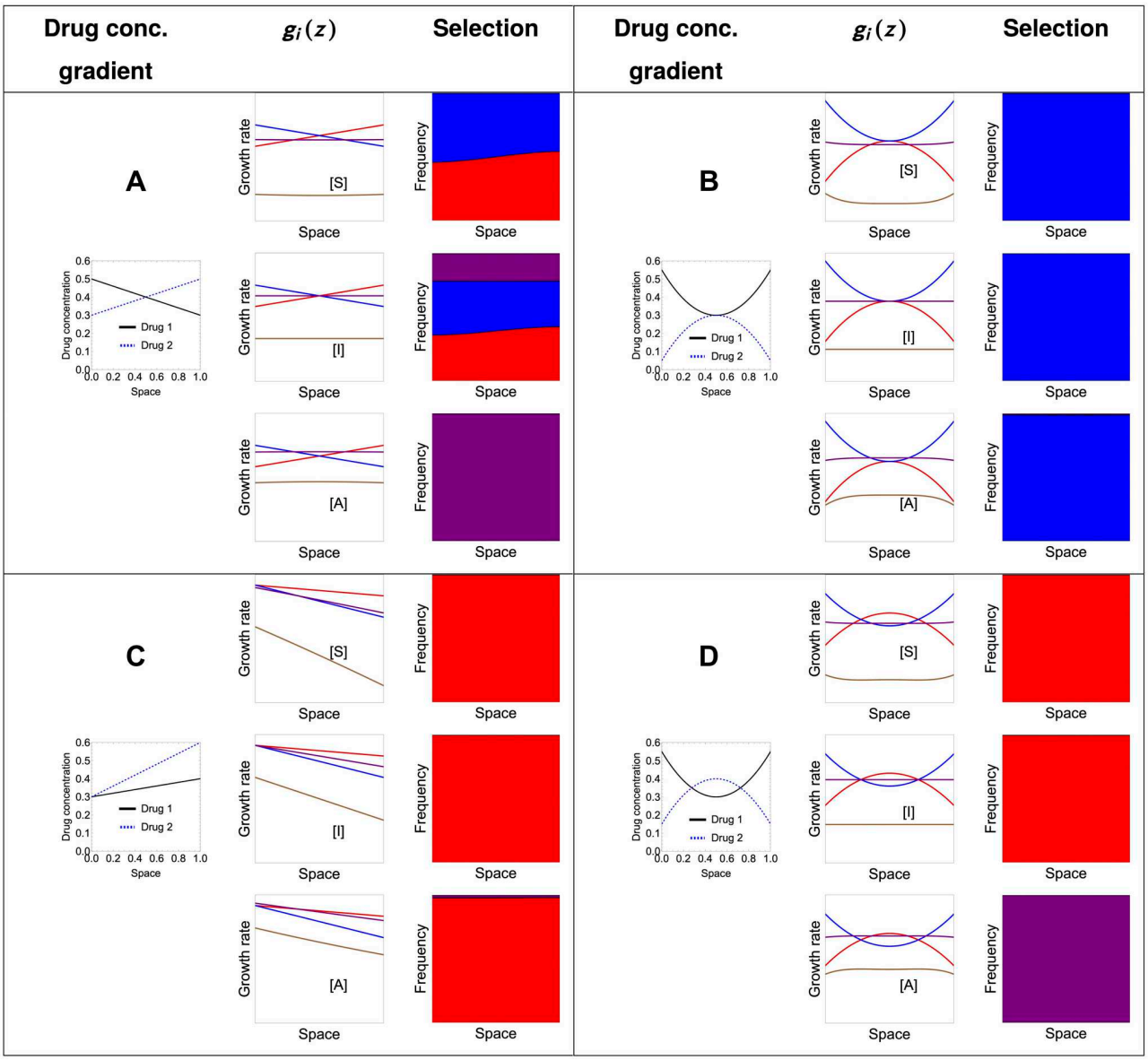

Fig 5. An atlas for 2-drug resistance evolution in space under spatial heterogeneity. We consider only four available mutants each with different resistance phenotypes to two drugs, distributed in the (α, β) space of rescaling parameters: blue—fully resistant to drug 1 and sensitive to drug 2; red—fully resistant to drug 2 and sensitive to drug 1; purple—intermediate resistance to both drugs; brown—wild-type, sensitive to both drugs. We considered a diffusion coefficient of $D = 0.01$; the spatial equilibrium is obtained numerically by considering the system at $t = 400$. For all the simulations, we considered the same initial distributions with 99% wild type mutants and the remaining 1% distributed equally among the three resistant mutants. The initial distributions of each mutant were shaped as the function $\sin\left(\frac{\pi z}{L}\right)$, so that the homogeneous Dirichlet boundary conditions were respected. The growth landscapes were as specified in Eq 16. The interaction strength is fixed at $q = 1$ both in the case of synergistic and antagonistic interaction. For more drug gradient scenarios, under a more complex drug interaction profile and two diffusion rates, see Supplementary Figs A-C in S1 Text.

https://doi.org/10.1371/journal.pcbi.1012098.g005

(Fig 5A), in the case of independent drugs, both mono-resistant and the double-resistant mutant coexist, in the case of antagonistic drugs, the intermediate double-resistant mutant has a higher chance to exclude the mono-resistant variants, and in the synergistic drugs regime, only the two mono-resistant mutants coexist. When one drug concentration exceeds the other drug concentration throughout the domain, as intuitively expected, the mutant that gets

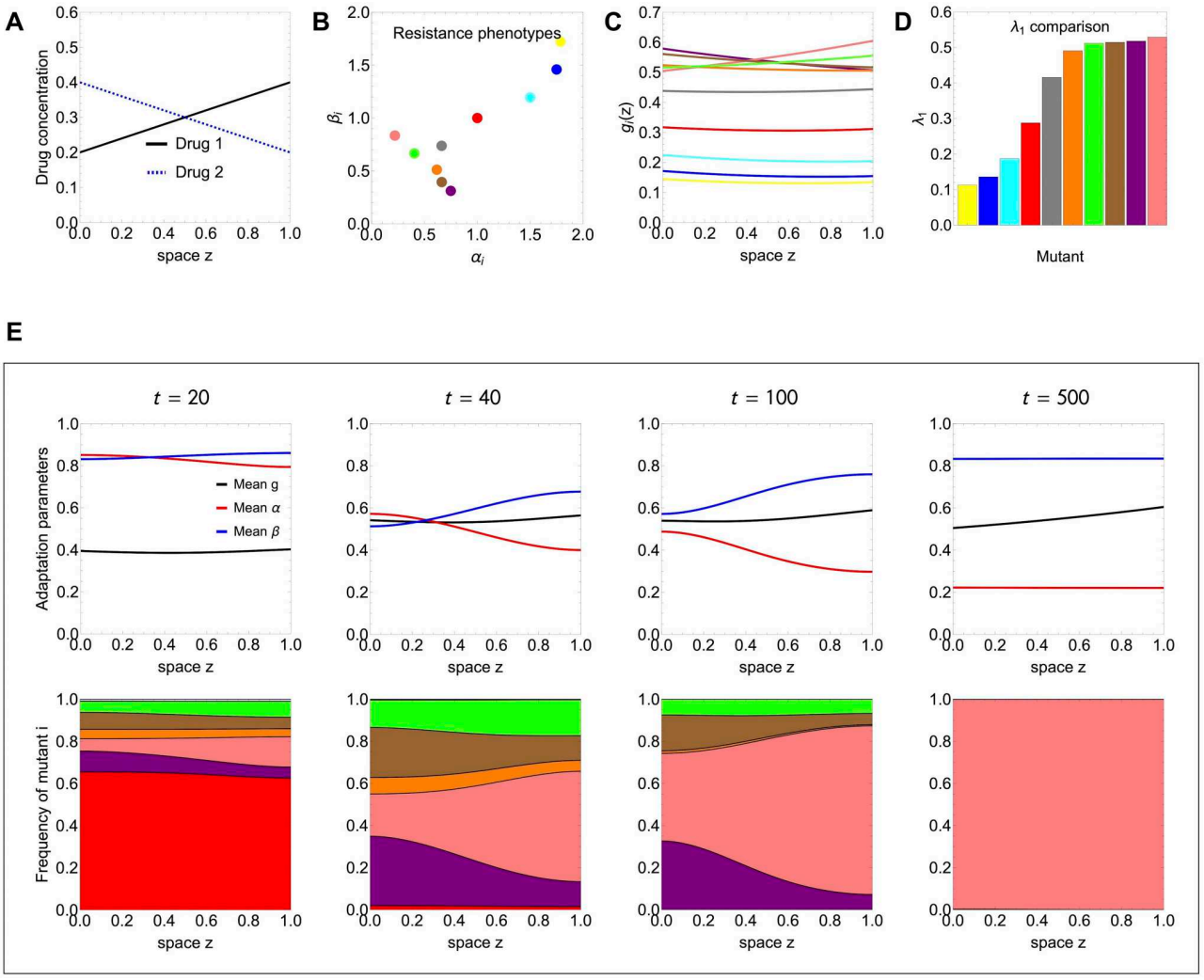

Fig 6. Validating selection predictions based on λ_1 ranking among several competing mutants. We illustrate a model simulation under the linear drug gradients in A, with 10 multi-drug resistant mutants varying in (α_i, β_i) traits (B), growing $(g_i(z)$ in C) and spreading over space with diffusion coefficient $D = 0.01$. The λ_1 values (Eq 14) in D, match very well with the spatial selection dynamics observed numerically (E). Initial conditions (99% vs 1%: WT vs. equal division among all the mutants) were assumed equal for all strains, satisfying the boundary conditions $n_i(z, 0) \sim sin(\pi z)$.

https://doi.org/10.1371/journal.pcbi.1012098.g006

selected in a competitive exclusion scenario uniformly over space, is the mutant that is resistant to that drug (Fig 5B and 5C). When the drugs co-vary in non-linear manner over space, depending on the way this gradient translates to relative growth functions among mutants, it is possible to have different selection scenarios and fine-tune parameters to invert the hierarchical competitive fitnesses of different types of resistance mutants (Fig 5D). Such selection outcomes can be entirely predicted analytically by computing and comparing the principal eigenvalues (Eq 14) between mutants in each case (see also S2 Mathematica Notebook and Supplementary Figs B-C in S1 Text).

Verifying predictions of selection over space based on λ_1

Next we show how the ranking based on λ_1 comparison between mutants gives accurate prediction for final outcome of competition over space in a more complex case with more

mutants ($M > 2$), more complex drug-interaction function, and arbitrary distribution of resistance phenotypes (see Fig 6).

Selection over space under motility and growth differences among mutants

A direct extension of this model is to, instead of assuming an equal D, allow for mutant-specific diffusion rates D_i, in the environment. In this case, there is an additional trait affecting global fitness over space, namely motility. In the case of constant growth rates g_i it is straightforward to obtain the fittest mutant by their ranking on the classical critical criterion $L_{crit} = \pi\sqrt{\frac{D_i}{g_i}}$ (also related to λ_1). The mutant with the smallest $L_{crit} < L$ should win. When two mutants have exactly the same fitness, perhaps by counter-balancing growth and diffusion, leading to same L_{crit} (equivalently same λ_1) they will coexist. Whereas in the case of spatially-varying growth rates $g_i(z)$, one can resort to the same principal eigenvalue approach and compute the mutant fitness by including the assumption of a different D_i for each mutant. In both these cases, the diffusion traits play a key role in determining the winner or coexistence in the system, with fast diffusion sometimes being able to rescue locally maladapted strains, or slow diffusion sometimes amplifying the fitness of lower-growth variants (see Section D in S1 Text and S3 Mathematica Notebook in Supplements). These theoretical predictions, made accessible here through the λ_1 comparison between variants, could be linked with existing empirical observations on bacterial coexistence and inverted competitive hierarchies driven by motility and spatial competition [88].

The case of periodic habitat quality: Periodic multi-drug regimes

A special case of environmental variation is periodic habitat quality; in the case of multi-drug regimes, this translates to periodically-varying drug concentrations in space. This case has been long studied in the theoretical ecology literature, for example for finite one-dimensional or two-dimensional space, or infinite one-dimensional environment [89, 90]. Typically a discretization approach is used, dividing the landscape into periodically-alternating patches of two or more types. In our case, such alternation of the space into patches of differential suitability for growth comes as a result of fitness being a direct function of the two drug concentrations. Namely for drug concentrations varying periodically in space:

$$x(z) = k_1 + A_1 \sin\left(\frac{2\pi z}{T_1}\right) \quad \text{and} \quad y(z) = k_2 + A_2 \sin\left(\frac{2\pi z}{T_2}\right),$$

where A_1 and A_2 denote the amplitude of spatial variation and T_1 and T_2 the period of the variation for each drug, the growth rate at each point in space of the wild-type (reference strain) would be given by

$$g_0(z) = G\Big(x(z), y(z)\Big)$$

and in general, the growth rate of any variant with resistance traits (α_i, β_i), would be given by

$$g_i(z) = G\Big(\alpha_i x(z), \beta_i y(z)\Big).$$

We consider again the simple drug landscapes G specified in Eq 16, where with a single parameter $q > 0$, we can vary the strength of the drug interaction. Focusing on three classical

mutants with traits (0, 1), (1, 0), and (0.5, 0.5), and computing their fitness based on the principal eigenvalue approach we can study which type of resistance, whether resistance to drug 1, or to drug 2 or intermediate resistance to both drugs will be favoured in each periodic drug regime, and how the result depends on the type and strength of drug interaction.

Indeed we see that for a given periodic variation of drugs over space, leading to a periodic variation of g over space, typically one mutant has the highest fitness. The theory predicts that under Dirichlet boundary conditions, and fixed mean growth rate over space, the population whose growth function exhibits the highest amplitude of variation, will be the one to win [89, 90], e.g. the mutant who experiences a less fragmented habitat. This result is not immediately translatable to our case, since what we are controlling for is not average growth rate of each mutant, but total amount of drug 1 and total amount of drug 2.

In our simulations with given parameters, when mean growth rates of mutants may vary, we find that the mutant with resistance to drug 1 is selected in Fig 7 top panels). However, as drug interactions increase in magnitude, the intermediate double-resistant mutant can be selected (Fig 7 last panel). These outcomes of selection cannot simply be understood from just comparing the amplitude and frequency of variation in $g(z)$, but also crucially on the mean growth rate that may change as we vary the two drugs or their interaction. In any case, computing the relative fitnesses on the basis of the principal eigenvalue ranking (see S4 Mathematica Notebook for this periodic case in the supplements), leads to robust analytical results, which can be extended to account for arbitrary environmental variation and coupling from environment to fitness.

Open avenues for multi-drug optimization over space

Keeping the total amount of each drug constant and equal when integrated over space, one can then try to perform optimization of periodic drug administration over space so as to select one or the other mutant. For the purposes of illustration, since detailed optimization falls beyond the scope of this paper, we studied systematically how the winning mutant varies depending on the period of a single drug's administration over space (Fig 8), and as a function of both drugs' spatial periods (Fig 9), in the three cases of synergistic, antagonistic and no-drug interaction. In our parameter combinations, we observe that the synergistic and independent drug actions produce very similar selection outcomes for any combination of periods of the two drugs between 0 and 2, always favouring single resistance to one drug, albeit overturning the winning strain for some critical parameter thresholds.

In contrast, the antagonistic drug scenario is the one that can lead also to relatively more selection of the intermediate double resistant mutant (Fig 8C relative to Fig 8A and 8B), and does so in a majority of parameter combinations (purple region in Fig 9C). This confirms that antagonistic drug combinations, even considering spatial variation, typically constrains high-level single resistance selection, in favour of the intermediate double resistance.

Although there appears to be little to no difference between the cases of synergistic and independent drugs, this has to do with the specific simple G functional forms used in this particular simulation (Eq 16) and the particular choice of extreme mutants (Fig 4). Since one of the parameters in the mutants is 0, then the $-qxy$ term vanishes in the synergistic case, making the generalist mutant suffer a disadvantage in the synergistic landscape.

Notice that two scenarios displaying the same final selection outcome only means that the ranking of the principal eigenvalues produces the same fittest strain; this does not preclude differences in the transient dynamics leading up to that outcome. Coexistence is obtained when strain fitness computed from the λ_1 is equal. Sometimes 2 mono-resistant strains may coexist excluding the double resistance (orange border line in Fig 9A), or the double resistant with a

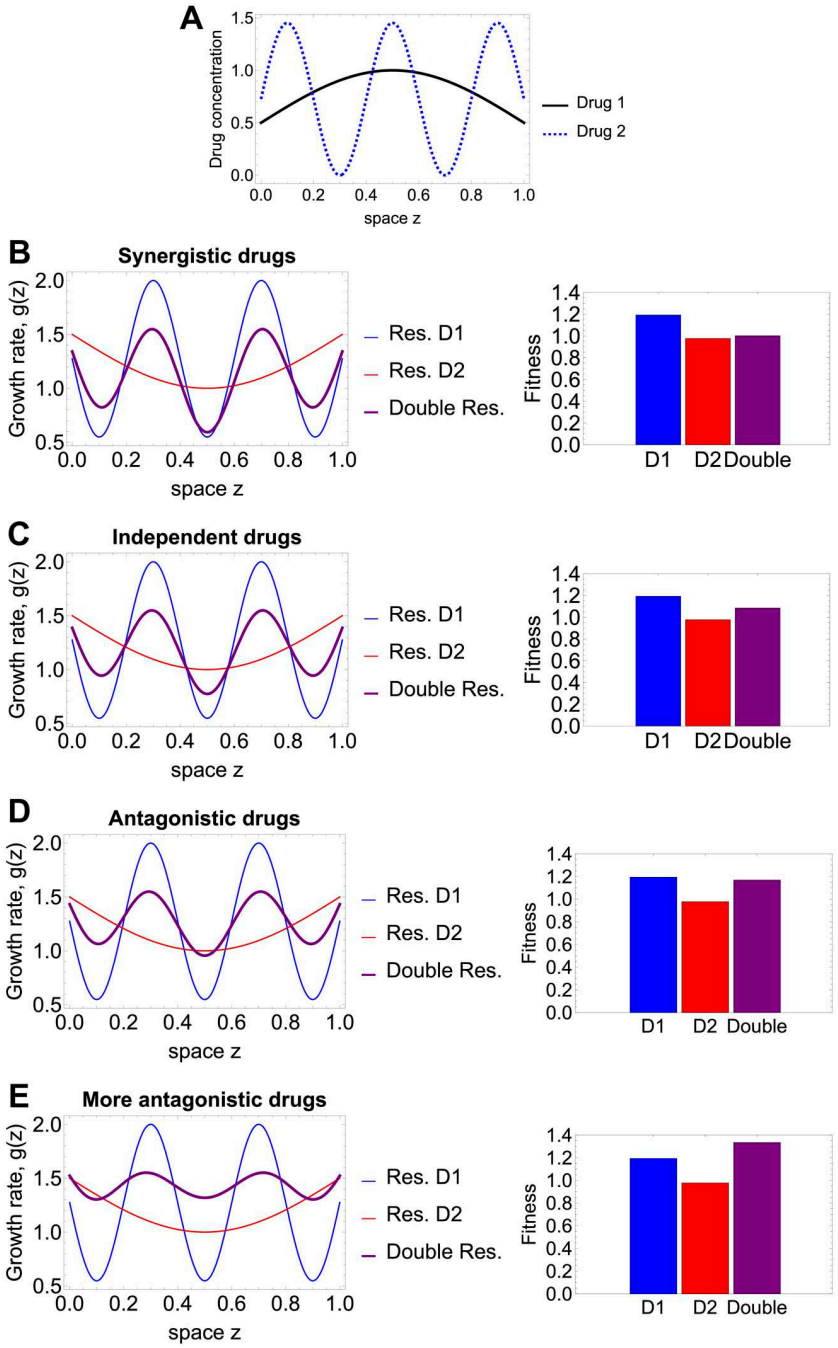

Fig 7. Selection outcomes for periodic drug regimes leading to periodic growth rates over space. A. The periodic variation of drug 1 and drug 2 over space, keeping the total amount of each drug equal. The periodic function parameters, under conservation of total drug, are: $k_1 = A_1 = 0.5$, $T_1 = 2$ and $k_2 = A_2 = 0.72$, $T_2 = 0.4$. Further we show mutant growth rates and selection outcome following the linear G function combinations in Eq 16 under: **B.** synergistic drug interactions (strength $q = 0.5$); **C.** independent drugs; D. antagonistic drug interactions (strength $q = 0.5$); **E.** even more antagonistic drugs (strength $q = 1.5$). The first column shows resulting growth rates $g_i(z)$ for each mutant. The second column shows associated principal eigenvalues for each of the 3 mutants over space, computed as an indicator of overall fitness where D1 refers to the mutant resistant to drug 1, D2 the mutant resistant to drug 2 and Double, the mutant partially resistant to both drugs. Assumed diffusion coefficient is $D = 0.01$. (See also S4 Mathematica Notebook for this case).

https://doi.org/10.1371/journal.pcbi.1012098.g007

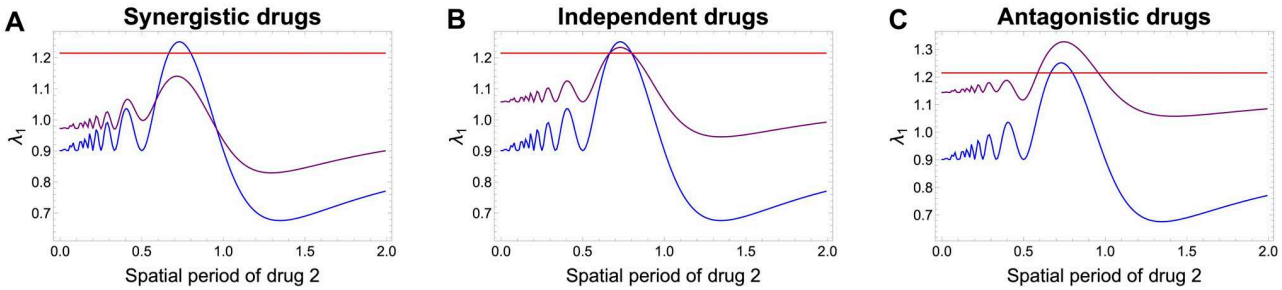

Fig 8. Fitness ranking among 3 mutants for periodic drug regimes, as a function of spatial period of drug 2. A. Synergistic drug interaction. **B.** Independent drug action **C.** Antagonistic drug interaction. The strength of interaction when assumed, was $q = 0.5$ and $G(x, y)$ were specified as in Eq 16. The periodic variation of drug 1 $x(z)$ was held fixed, while drug 2 concentration $y(z)$ over space was varied by varying the period T_2. These parameters were fixed: $k_1 = A_1 = 0.5$, $T_1 = 0.8$ and $k_2 = A_2 = 0.5$ before normalization, which then leads to total conservation of drug 1 and drug 2, fixed amount = 1 for each spatial period of drug 2 T_2. Final fitnesses of the 3 mutants over space, computed on the basis of the principal eigenvalue. Assumed diffusion coefficient is $D = 0.01$. In blue: single-resistance to drug 1, in red: single-resistance to drug 2, in purple: double resistant mutant with intermediate resistance to each drug.

https://doi.org/10.1371/journal.pcbi.1012098.g008

single mono- resistant strain (region border lines in Fig 9C), and under independent drugs, 3 strains can coexist including both mono-resistant and the double resistant strains (green border line in Fig 9B).

In contrast, the use of the spatially-averaged growth rates in these scenarios as a proxy to predict selection would yield very different results to λ_1. With the drug landscape defined in 16 and the total amount of the two drugs equal, we would have only one possible outcome under each drug interaction, independently of periods (T_1, T_2). Namely, in the synergistic case we would always have coexistence of the mono-resistance mutants, in the independent drug action case, coexistence of the three mutants (both single-resistant and the double-resistant

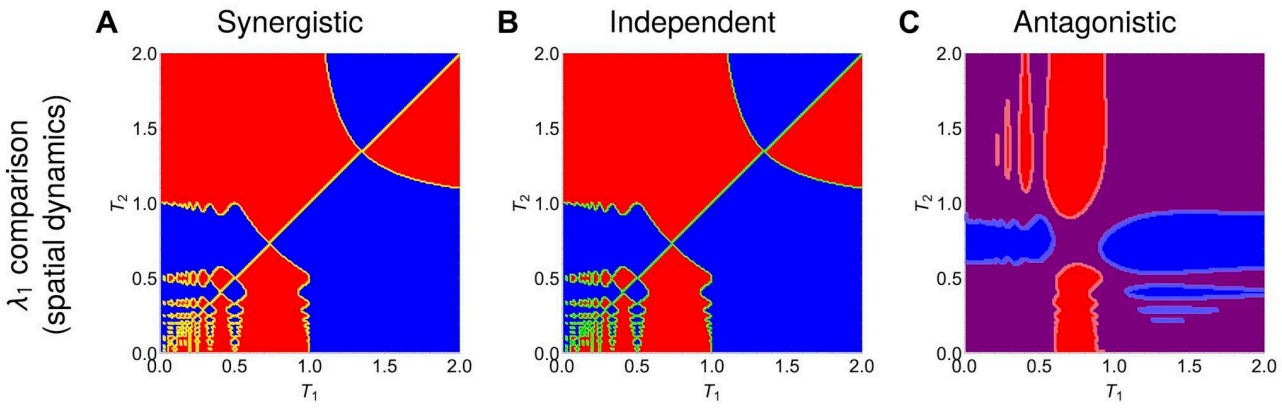

Fig 9. Drug-resistance selection outcomes for periodic 2 drugs as a function of their spatial periods T_1 and T_2. A. Synergistic drugs. **B.** Independent drugs. **C.** Antagonistic drugs. Shaded blue region: single-resistance to drug 1 has higher fitness, shaded red region: single-resistance to drug 2 has higher fitness, shaded purple region: double resistant mutant with intermediate resistance to each drug has the higher fitness. The periodic variations of drug 1 and drug 2 over one-dimensional space $z \in [0, 1]$ are constructed in such way as to keep the total amount of each drug equal to 1. The periodic function parameters are initially specified as: $k_1 = A_1 = k_2 = A_2$ for any combination of periods T_1 and T_2, and then immediately scaled by the integral of the periodic function over space, to obtain a total amount of drug equal to unity in each case. Assumed diffusion coefficient is $D = 0.01$. The growth functions of each mutant over space are obtained following Eqs. 16 together with the assumption that a mutant with traits (α_i, β_i) experiences the two drugs at concentrations $\alpha_i x$ and $\beta_i y$. The interaction strength is fixed at $q = 0.5$ both in the case of synergistic and antagonistic interaction. In the case of synergistic/antagonistic interaction, the effect is to decrease/increase the growth rate of bacteria relative to the simple additive effect of the two drugs. See Fig D (S1 Text) for the analogous figure under a more complex drug interaction function, highlighting the sensitivity to fitness landscape.

https://doi.org/10.1371/journal.pcbi.1012098.g009

mutant have equal $\bar{g}$), and under antagonistic drugs, the double-resistant mutant with intermediate resistance to both drugs would competitively exclude the other mutants. This result could be easily verified analytically via the integrals $\bar{g} = \int_0^L g(z)dz$ which would lead to the following growth rates:

$$\bar{g}_{(1,0)} = \int_0^L 2 - x(z)dz = \bar{g}_{(0,1)} \int_0^L 2 - y(z)dz > \bar{g}_{(0.5,0.5)} = \int_0^L \left[2 - \frac{x(z) + y(z)}{2} - \frac{q}{4}x(z)y(z)\right]dz$$

- from the assumption of total drug amount being equal $\int_0^L xdz = \int_0^L y(z)dz$, and noting $q > 0$. Hence, for whichever variation of x and y over space (i.e. independently of T_1 and T_2), the single-drug resistances would be selected.

The explicit analytical handle on relative fitness based on λ_1 could further be used to design optimal multi-drug regimes over space under certain constraints. For example, fixing the total amount of drug 1, and its spatial variation, which total amount of drug 2 and spatial variation would be needed to drive the double-resistant mutant toward extinction ($\lambda_1 < 0$)? In Fig E (S1 Text) we illustrate an answer to this question, identifying precisely those drug-2 gradients over space that would be effective. Further analytical advances in multi-drug therapeutic optimization over spatially extended habitats could be obtained, by exploiting previous theoretical results [85, 90, 91] and linking them to antibiotics and bacterial realities, or generating new results on a case-by-case basis for specific cell populations under spatial gradients.

Discussion

The spatiotemporal evolution of strain frequencies in a population spreading in a homogeneous environment can be described by parallel travelling fronts where each strain propagates in space with a constant speed, according to the classical Fisher-KPP equation [80, 81]—an equation with a long history of study in biological invasions and population genetics [84, 92]. Under the classical exponential or logistic growth kinetics, the result of such competition typically leads to competitive exclusion where the fittest strain will be the only one to survive everywhere in space over long time.

In a spatially-varying environment, the local quality of the habitat affects the speed of spread of an invading population. Natural environments where populations grow and spread are generally heterogeneous, composed of different sub-habitats, such as forests, plains, marshes, and the like, or consist of fragments divided by barriers such as roads, rivers, cultivated fields [93]. This case has a long history of ecological, environmental and agricultural interest, and a long history of mathematical study with analytical results on periodic traveling waves [94], piecewise-environmental variation [85] and up to the more recent work by [89, 90] on periodic spatial variation, with the pulsating front characterized by its average speed.

The key quantity highlighted in many of these earlier studies is the principal eigenvalue of the linearized equation, which determines the global stability of the stationary state 0. Although these studies were primarily interested in biological invasion of a single species, such result can be applied to the context of multiple strains of a population spreading in a heterogeneous habitat. One can make use of the same logic, for ranking the fitness of different mutants on such heterogeneous habitat, or alternatively for determining relative environmental suitability for each mutant. Ranking the global (in)stability of the 0 steady state, via principal eigenvalue comparisons, allows to reach a conclusion about the strains' survival in an environment that is differentially suitable, and hence predict selection outcomes in the system over long time.

Harnessing the analytical foundations of these results, we go here one step further by applying this theory to the context of antibiotic resistance evolution, by proposing λ_1 as a metric for

global mutant fitness to predict multi-resistance selection under multi-drug environmental gradients, and by providing an accurate approximation of this principal eigenvalue. We study arbitrary variation in the environment suitability, linking spatial heterogeneity to explicit multi-drug antibiotic regimes, and integrating fitness landscapes, drug interactions and collateral effects, with the aim to predict multi-drug resistance evolution as a selection process among any mutants. Other studies have considered the role of spatial heterogeneity in the evolution of resistance, using the framework of an epidemiological model and focusing on the case of a single drug being used with periodic variation in the growth rates of single and double-resistant genotypes [95]. Here we develop a more general and comprehensive link between traveling fronts and multi-drug resistance. In our framework, periodic variation can be seen as a special case of spatial heterogeneity, when drugs are used at periodic concentrations over space. Furthermore, differently from [95], we include the possibility of multiple drugs interacting, which affects mutant success and final competitive outcome between multi-drug resistant variants.

The main advantage of this framework is that it provides a simple and general template for studying multi-drug resistance evolution in space, possibly applicable to other systems and open to analytical extensions (Box 3). In particular, it allows for continuous resistance traits, includes collateral effects and drug interactions explicitly, and the prediction of final outcomes is based on dominant eigenvalue ranking among mutants, which can be analytically approximated. The framework is easily extendable to include spatial variation of multiple drugs to >2 drugs, and hence enabling study of higher-dimensional evolution in antibiotic resistance fitness traits. Especially in the case of 1-d and 2-d environments, there are many results that can be directly applied from the literature to the case of antibiotic resistance, such as optimal spatial variation to prevent or facilitate global spread of an invading species or strain [85, 89].

Mathematically, and strictly-speaking the λ_1 presented in our framework corresponds to a growth rate, related to the negative principal eigenvalue in other studies [85, 89, 91], whose optimization for invasion and persistence would seek a minimum. While this is a convention, our technical choice enables us conceptually and practically to rank the mutants more easily favouring the one with the relatively higher λ_1. Other approaches to compute or obtain suitable bounds for λ_1 can come from variational methods applied to Sturm-Liouville problems and the Rayleigh quotient [96]. We adopted a perturbation theory approach, which despite its requirement for ϵ small, appears to apply well outside this immediate strict range. In particular, the λ_1 approximation matches very well the selection results that the model simulations display even in cases of lower diffusion.

While in many models of evolution dynamics, fitness is typically represented by the mutant growth rate, here we emphasize that under spatial dynamics, mutant fitness is not given simply by g_i or spatial averages thereof, but rather by the corresponding value of λ_1. The exact expression of this principal eigenvalue will depend on the boundary conditions. In the case of Dirichlet boundary conditions, considered here, the spatial growth rate enters λ_1 via a weighting factor $sin^2\left(\frac{\pi z}{L}\right)$. In section E of S1 Text we show that in the case of Neumann (no-flux) boundary conditions, the growth rate enters the λ_1 simply as a spatially-averaged growth rate. Whereas in the case of mixed-boundary conditions, the weighting factor for $g(z)$ is $sin\left(\frac{\pi z}{2L}\right)$. This ultimate dependence of fitness on the type of boundary condition can lead naturally to different selection outcomes, as illustrated in Fig F in S1 Text where 2 mutant growth rates vary spatially as in Fig 2A but boundary conditions are of 3 types.

Our results are strictly limited to non-interacting populations growing exponentially–an assumption that both simplifies the analysis and allows us to interpret the λ_1 as experimentally accessible parameter: an effective growth rate. However, many of these results may be valid in

Box 3. General applicability of the framework, outlook and challenges

Spatial growth and selection under multiple stressors

The simple framework based on rescaling parameters (α, β) could be applied to other biological populations, at different scales, growing in response to multiple stressors and spreading through migration in heterogeneous environments that generate a gradient for growth (see figure below in this box). Differential variant makeup, whether genetic or non-genetic, but heritable, that produces different susceptibility traits to these stressors in the population forms the basis for selection on relevant timescales, manifested in its simplest form as competitive exclusion (*monomorphism*) or coexistence patterns (*polymorphism*) in spatially extended habitats. The stressors could range from antibiotics [99], to agrochemicals [100], temperature, moisture, [101], pH, salinity [102], to nutrient levels, oxygen, or physiological micro-environments [24].

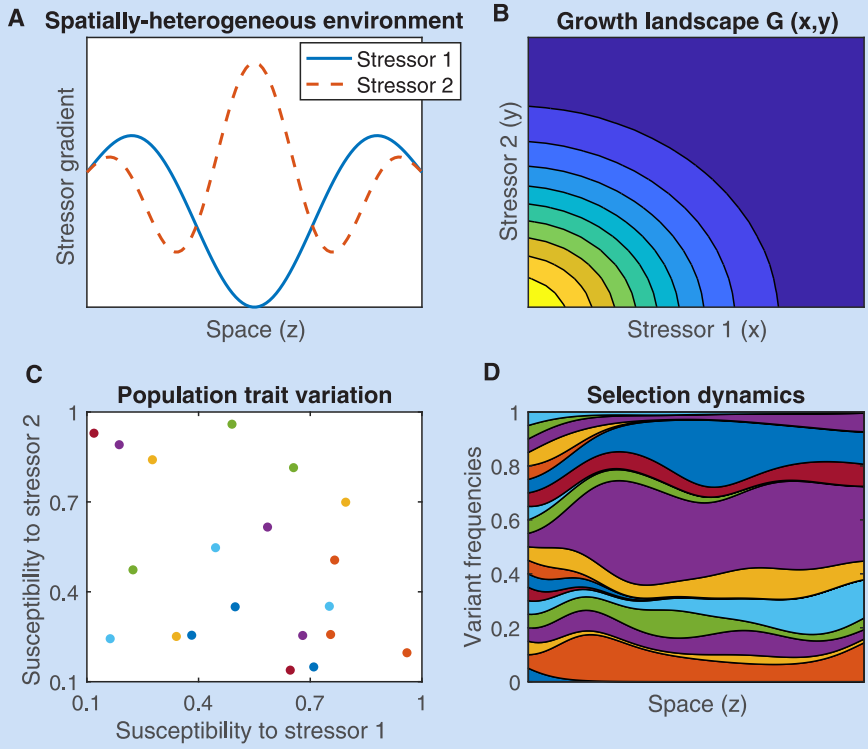

Model translation to environmental contexts beyond antibiotics. A. *Two arbitrary spatially-varying stressors (1 and 2).* **B.** *The growth landscape G(x, y) of the reference (WT) strain as a function of stressor concentrations forms the basis for building later the growth landscapes of different mutants.* **C.** *The primary dose-responses of stressor- to- growth phenotypic effect can be used to obtain (α_i, β_i) traits in the sub-populations of interest.* **D.** *These coefficients are then used to rescale G accordingly to obtain growth rates $g_i(z)$ for all variants under various stressor concentrations. With these ingredients, the model can be applied to other ecological contexts.*

Limitations and caveats

In some cases, scaling factors may not fully capture the variation in mutant growth relative to wild-type as a function of stressor concentrations. Much more nonlinear functional transformations may be required to obtain mutant fitness landscapes, and this remains an active area of research [87]. Similarly, the exponential model may be too unrealistic to represent the intricate mechanisms of growth and interactions between strains [103, 104], thusfar assumed negligible. We focused on the case of mainly positive growth rates. However, locally negative growth rates (e.g. supra-inhibitory stressor doses) could complicate outcomes, via stronger dependence on initial conditions, or additional sensitivity to variable diffusion rates to compensate for fitness troughs.

Extensions and outlook

Applications can be envisaged in other systems such as gut microbiota, soil bacteria and their spatio-temporal distribution under abiotic gradients, cancer cell populations and drug resistance selection dynamics along physiological gradients, antibiotic resistance evolution at the epidemiological scale, toxicology data, freshwater aquatic systems and environmental biotechnology. More than 2 stressors could be implemented, thereby yielding high-dimensional susceptibility traits. An additional axis of resistance cost can be integrated, either as independent or via a functional dependence on α, β traits. The model could include space-dependent diffusion or habitat preference bias at the interface between distinct environmental patches [103]. Analytical extensions could exploit links with homogenization techniques from landscape ecology [105] and global fitness perspectives from adaptive dynamics [106].

other growth regimes, particularly in cases where competition manifests itself as a growth limitation that uniformly impacts all mutants (e.g. logistic growth), a regime that has been the focus of much of the foundational work on spatial heterogeneity [85, 96]. From a technical perspective, the nonlinearities introduced by different growth regimes are likely to require differences in approach and interpretation–for example, by restricting the interpretation of the principal eigenvalue to a somewhat abstract indicator of the stability of particular fixed points rather than a simple measurable observable (growth rate). Nevertheless, the past success of similar approaches, along with the empirical evidence that simple non-interacting models may have predictive power both in considerably more complex laboratory and in-silico situations (e.g. [79]), leads us to speculate that qualitatively similar dynamics might be expected in a wider range of systems.

A disadvantage of our approach is that while the population involved and its constituent strains are considered dynamic, the environment, namely the drug concentrations across space, is generally regarded as static. Other modeling frameworks are needed to treat situations with both temporal and spatial variation in the environment, or a mutual feedback, such as in resource-based models where cells physically interact with resources at the expanding front, e.g. in biofilms [97, 98]. Similarly, by assuming large populations, we neglect stochastic fluctuations in sub-populations which might affect selection outcomes in certain settings.

We only included diffusion, i.e. random movement of cells in space, while other similar reaction-diffusion models focusing on microbiota composition variation along the gut have

included both diffusion and directed flow of bacterial lineages along a longitudinal growth gradient (see [107] and [108–110]). We also did not explicitly include active mutation processes in the kinetics of the spatial model, a process which would break the independence between the existing strains [70], and preclude the straightforward application of the first eigenvalue approach for fitness comparison. In the particular case in which mutation rates to a given variant are equal among all possible parental strains, one could plausibly assume the initial total distribution among mutants as a proxy for such hierarchical mutation biases, and apply still the present model. *De-novo* diversity generation could be added with specific assumptions on parent and offspring phenotypes, dependence on the current environment, population size, and/or spatially-varying mutation rate. This remains an interesting avenue for the future.

Another mechanism to break the independence between sub-populations would be competition or facilitation between variants, explicitly embedded into their growth kinetics and spatial spread. Other studies have addressed it e.g. in ecological models [103, 104] or epidemiological multi-strain systems [111, 112], leading to potentially very complex replicator-type equations with frequency-dependent fitness and dynamics extended to space. Although we did not focus on analytical results for coexistence levels between strains, when their global fitnesses equalized over space, these results can be easily obtained from the same approximation steps based on perturbation, that allowed us to compute the dominant eigenvalue for each mutant (see S1 Text Sections A-D). On the other hand, analytical results for total population size and frequencies could be more easily obtained for cases with constant growth rates over space, applying classical reaction-diffusion theory and travelling-wave characterization of the solutions.

While the debate of antibiotic resistance management [113] has optimization at the center, we very briefly sketched a few aspects of the model to inform optimal combination multi-drug therapies over space (e.g. Fig 9 and E in S1 Text). Analytical results on optimization remain challenging even for simple piecewise growth variation as recognized in earlier work [85]. Many factors do play a role, including sensitivity to boundary conditions and structure of habitat fragmentation [89, 91], modelling assumptions, nonlinearities linking phenotypes to growth and variation in habitat 'quality', and details of underlying stressor interaction. However, the general framework presented here for multi-drug gradients can be a basis that can be tailored to specific systems and their optimal control in the future. We expect many opportunities for model-data links both in microbiology and lab evolution experiments, as well as in the larger-scale epidemiology of multi-drug resistance evolution.

Supporting information

S1 Text. Compiled supporting information. A single file with all supporting material text and figures, code and video captions.
(PDF)

S1 Video. Spatiotemporal dynamics of multi-drug resistant mutant selection over space leading to selection of the 'pink' mutant (scenario in Fig 6).
(GIF)

S2 Video. Spatiotemporal dynamics of multi-drug resistant mutant selection over space leading to selection of the 'purple' mutant (same scenario as Fig 6, but for higher diffusion rate of the 'pink' variant).
(GIF)

S1 Mathematica Notebook. Solutions of the PDE system (related to Fig 2 of the paper).
(TXT)

S2 Mathematica Notebook. Growth variation, principal eigenvalue and selection outcomes (related to Fig 5 of the paper).
(TXT)

S3 Mathematica Notebook. Principal eigenvalue and predicting selection (related to Fig 6 of the paper).
(TXT)

S4 Mathematica Notebook. Exploring periodic multi-drug regimes and λ_1 (related to Fig 7 of the paper).
(TXT)

Author Contributions

Conceptualization: Kevin B. Wood, Erida Gjini.

Formal analysis: Tomas Ferreira Amaro Freire, Zhijian Hu, Kevin B. Wood, Erida Gjini.

Funding acquisition: Tomas Ferreira Amaro Freire, Kevin B. Wood, Erida Gjini.

Investigation: Tomas Ferreira Amaro Freire, Zhijian Hu, Kevin B. Wood, Erida Gjini.

Methodology: Kevin B. Wood, Erida Gjini.

Project administration: Erida Gjini.

Resources: Kevin B. Wood, Erida Gjini.

Software: Tomas Ferreira Amaro Freire.

Supervision: Erida Gjini.

Validation: Zhijian Hu, Kevin B. Wood.

Visualization: Tomas Ferreira Amaro Freire, Erida Gjini.

Writing – original draft: Erida Gjini.

Writing – review & editing: Kevin B. Wood, Erida Gjini.

References

1. Laxminarayan R, Duse A, Wattal C, Zaidi AK, Wertheim HF, Sumpradit N, et al. Antibiotic resistance? the need for global solutions. The Lancet infectious diseases. 2013; 13(12):1057–1098. https://doi.org/10.1016/S1473-3099(13)70318-9 PMID: 24252483
2. Cassini A, Högberg LD, Plachouras D, Quattrocchi A, Hoxha A, Simonsen GS, et al. Attributable deaths and disability-adjusted life-years caused by infections with antibiotic-resistant bacteria in the EU and the European Economic Area in 2015: a population-level modelling analysis. The Lancet infectious diseases. 2019; 19(1):56–66. https://doi.org/10.1016/S1473-3099(18)30605-4 PMID: 30409683
3. Marston HD, Dixon DM, Knisely JM, Palmore TN, Fauci AS. Antimicrobial resistance. Jama. 2016; 316(11):1193–1204. https://doi.org/10.1001/jama.2016.11764 PMID: 27654605
4. Murray CJ, Ikuta KS, Sharara F, Swetschinski L, Aguilar GR, Gray A, et al. Global burden of bacterial antimicrobial resistance in 2019: a systematic analysis. The Lancet. 2022; 399(10325):629–655. https://doi.org/10.1016/S0140-6736(21)02724-0
5. Beardmore RE, Pena-Miller R, Gori F, Iredell J. Antibiotic Cycling and Antibiotic Mixing: Which One Best Mitigates Antibiotic Resistance? Molecular Biology and Evolution. 2017; 34(4):802–817. https://doi.org/10.1093/molbev/msw292 PMID: 28096304
6. Brown EM, Nathwani D. Antibiotic cycling or rotation: a systematic review of the evidence of efficacy. Journal of Antimicrobial Chemotherapy. 2005 01; 55(1):6–9. https://doi.org/10.1093/jac/dkh482 PMID: 15531594

7. Bergstrom CT, Lo M, Lipsitch M. Ecological theory suggests that antimicrobial cycling will not reduce antimicrobial resistance in hospitals. Proceedings of the National Academy of Sciences. 2004; 101 (36):13285–13290. https://doi.org/10.1073/pnas.0402298101

8. Nichol D, Jeavons P, Fletcher AG, Bonomo RA, Maini PK, Paul JL, et al. Steering evolution with sequential therapy to prevent the emergence of bacterial antibiotic resistance. PLoS Comput Biol. 2015; 11(9):e1004493. https://doi.org/10.1371/journal.pcbi.1004493 PMID: 26360300

9. Batra A, Roemhild R, Rousseau E, Franzenburg S, Niemann S, Schulenburg H. High potency of sequential therapy with only β-lactam antibiotics. Elife. 2021; 10:e68876. https://doi.org/10.7554/eLife.68876 PMID: 34318749

10. Gjini E, Brito PH. Integrating Antimicrobial Therapy with Host Immunity to Fight Drug-Resistant Infections: Classical vs. Adaptive Treatment. PLOS Computational Biology. 2016 04; 12(4):1–34. https://doi.org/10.1371/journal.pcbi.1004857 PMID: 27078624

11. Hansen E, Woods RJ, Read AF. How to use a chemotherapeutic agent when resistance to it threatens the patient. PLoS biology. 2017; 15(2):e2001110. https://doi.org/10.1371/journal.pbio.2001110 PMID: 28182734

12. Hansen E, Karslake J, Woods RJ, Read AF, Wood KB. Antibiotics can be used to contain drug-resistant bacteria by maintaining sufficiently large sensitive populations. PLOS Biology. 2020; 18(5):1–20. https://doi.org/10.1371/journal.pbio.3000713 PMID: 32413038

13. Gatenby RA, Silva AS, Gillies RJ, Frieden BR. Adaptive therapy. Cancer research. 2009; 69 (11):4894–4903. https://doi.org/10.1158/0008-5472.CAN-08-3658 PMID: 19487300

14. West J, You L, Zhang J, Gatenby RA, Brown JS, Newton PK, et al. Towards multidrug adaptive therapy. Cancer research. 2020; 80(7):1578–1589. https://doi.org/10.1158/0008-5472.CAN-19-2669 PMID: 31948939

15. Baym, Stone LK, Kishony R. Multidrug evolutionary strategies to reverse antibiotic resistance. Science. 2016; 351(6268):aad3292. https://doi.org/10.1126/science.aad3292 PMID: 26722002

16. MacLean RC, Hall AR, Perron GG, Buckling A. The population genetics of antibiotic resistance: integrating molecular mechanisms and treatment contexts. Nature Reviews Genetics. 2010; 11(6):405–414. https://doi.org/10.1038/nrg2778 PMID: 20479772

17. Holmes AH, Moore LS, Sundsfjord A, Steinbakk M, Regmi S, Karkey A, et al. Understanding the mechanisms and drivers of antimicrobial resistance. The Lancet. 2016; 387(10014):176–187. https://doi.org/10.1016/S0140-6736(15)00473-0 PMID: 26603922

18. Singer RS, Ward MP, Maldonado G. Can landscape ecology untangle the complexity of antibiotic resistance? Nature Reviews Microbiology. 2007; 5(1):82–82. https://doi.org/10.1038/nrmicro1593

19. Denk-Lobnig M, Wood KB. Antibiotic resistance in bacterial communities. Current Opinion in Microbiology. 2023; 74:102306. https://doi.org/10.1016/j.mib.2023.102306 PMID: 37054512

20. Lane PG, Hutter A, Oliver SG, Butler PR. Selection of Microbial Mutants Tolerant To Extreme Environmental Stress Using Continuous Culture- Control Design. Biotechnology progress. 1999; 15(6):1115–1124. https://doi.org/10.1021/bp990084j PMID: 10585198

21. Kawecki TJ, Lenski RE, Ebert D, Hollis B, Olivieri I, Whitlock MC. Experimental evolution. Trends in ecology & evolution. 2012; 27(10):547–560. https://doi.org/10.1016/j.tree.2012.06.001 PMID: 22819306

22. Hughes D, Andersson DI. Evolutionary trajectories to antibiotic resistance. Annual Review of Microbiology. 2017; 71:579–596. https://doi.org/10.1146/annurev-micro-090816-093813 PMID: 28697667

23. Donaldson GP, Lee SM, Mazmanian SK. Gut biogeography of the bacterial microbiota. Nature Reviews Microbiology. 2016; 14(1):20–32. https://doi.org/10.1038/nrmicro3552 PMID: 26499895

24. Chikina A, Vignjevic DM. At the right time in the right place: how do luminal gradients position the microbiota along the gut? Cells & Development. 2021; 168:203712. https://doi.org/10.1016/j.cdev.2021.203712 PMID: 34174490

25. Hanski I. Metapopulation dynamics. Nature. 1998; 396(6706):41–49. https://doi.org/10.1038/23876

26. Nicoletti G, Padmanabha P, Azaele S, Suweis S, Rinaldo A, Maritan A. Emergent encoding of dispersal network topologies in spatial metapopulation models. Proceedings of the National Academy of Sciences. 2023; 120(46):e2311548120. https://doi.org/10.1073/pnas.2311548120 PMID: 37931096

27. Thomas LJ, Huang P, Yin F, Luo XI, Almquist ZW, Hipp JR, et al. Spatial heterogeneity can lead to substantial local variations in COVID-19 timing and severity. Proceedings of the National Academy of Sciences. 2020; 117(39):24180–24187. https://doi.org/10.1073/pnas.2011656117 PMID: 32913057

28. Zulu LC, Kalipeni E, Johannes E. Analyzing spatial clustering and the spatiotemporal nature and trends of HIV/AIDS prevalence using GIS: the case of Malawi, 1994-2010. BMC infectious diseases. 2014; 14(1):1–21. https://doi.org/10.1186/1471-2334-14-285 PMID: 24886573

29. Feder AF, Harper KN, Brumme CJ, Pennings PS. Understanding patterns of HIV multi-drug resistance through models of temporal and spatial drug heterogeneity. Elife. 2021; 10:e69032. https://doi.org/10.7554/eLife.69032 PMID: 34473060

30. Silva J, Fariñas M, Felfili J, Klink C. Spatial heterogeneity, land use and conservation in the cerrado region of Brazil. Journal of biogeography. 2006; 33(3):536–548. https://doi.org/10.1111/j.1365-2699.2005.01422.x

31. Hovick TJ, Elmore RD, Fuhlendorf SD, Engle DM, Hamilton RG. Spatial heterogeneity increases diversity and stability in grassland bird communities. Ecological Applications. 2015; 25(3):662–672. https://doi.org/10.1890/14-1067.1 PMID: 26214912

32. Allen B, Lippner G, Chen YT, Fotouhi B, Momeni N, Yau ST, et al. Evolutionary dynamics on any population structure. Nature. 2017; 544(7649):227–230. https://doi.org/10.1038/nature21723 PMID: 28355181

33. Marrec L, Lamberti I, Bitbol AF. Toward a universal model for spatially structured populations. Physical review letters. 2021; 127(21):218102. https://doi.org/10.1103/PhysRevLett.127.218102 PMID: 34860074

34. Constable GW, McKane AJ. Fast-mode elimination in stochastic metapopulation models. Physical Review E. 2014; 89(3):032141. https://doi.org/10.1103/PhysRevE.89.032141 PMID: 24730823

35. Lieberman E, Hauert C, Nowak MA. Evolutionary dynamics on graphs. Nature. 2005; 433(7023):312–316. https://doi.org/10.1038/nature03204 PMID: 15662424

36. Kreger J, Brown D, Komarova NL, Wodarz D, Pritchard J. The role of migration in mutant dynamics in fragmented populations. Journal of Evolutionary Biology. 2023; 36(2):444–460. https://doi.org/10.1111/jeb.14131 PMID: 36514852

37. Chakraborty PP, Nemzer LR, Kassen R. Experimental evidence that metapopulation structure can accelerate adaptive evolution. bioRxiv. 2021;.

38. Korolev KS, Avlund M, Hallatschek O, Nelson DR. Genetic demixing and evolution in linear stepping stone models. Reviews of modern physics. 2010; 82(2):1691. https://doi.org/10.1103/RevModPhys.82.1691 PMID: 21072144

39. Korolev KS. The fate of cooperation during range expansions. PLoS Comput Biol. 2013; 9(3):e1002994.

40. Korolev KS. Evolution arrests invasions of cooperative populations. Physical review letters. 2015; 115(20):208104. https://doi.org/10.1103/PhysRevLett.115.208104 PMID: 26613477

41. Datta MS, Korolev KS, Cvijovic I, Dudley C, Gore J. Range expansion promotes cooperation in an experimental microbial metapopulation. Proceedings of the National Academy of Sciences. 2013; 110(18):7354–7359. https://doi.org/10.1073/pnas.1217517110

42. Sharma A, Wood KB. Spatial segregation and cooperation in radially expanding microbial colonies under antibiotic stress. The ISME Journal. 2021; 15(10):3019–3033. https://doi.org/10.1038/s41396-021-00982-2 PMID: 33953363

43. Martínez-Calvo A, Trenado-Yuste C, Lee H, Gore J, Wingreen NS, Datta SS. Interfacial morphodynamics of proliferating microbial communities. bioRxiv. 2023;Available from: https://www.biorxiv.org/content/early/2023/10/24/2023.10.23.563665 PMID: 37961366

44. Atis S, Weinstein BT, Murray AW, Nelson DR. Microbial range expansions on liquid substrates. Physical review X. 2019; 9(2):021058. https://doi.org/10.1103/PhysRevX.9.021058

45. Plummer A, Benzi R, Nelson DR, Toschi F. Fixation probabilities in weakly compressible fluid flows. Proceedings of the National Academy of Sciences. 2019; 116(2):373–378. https://doi.org/10.1073/pnas.1812829116 PMID: 30587586

46. Brockhurst MA, Rainey PB, Buckling A. The effect of spatial heterogeneity and parasites on the evolution of host diversity. Proceedings of the Royal Society of London Series B: Biological Sciences. 2004; 271(1534):107–111. https://doi.org/10.1098/rspb.2003.2556 PMID: 15002778

47. Campos PR, Neto PS, De Oliveira VM, Gordo I. Environmental heterogeneity enhances clonal interference. Evolution: International Journal of Organic Evolution. 2008; 62(6):1390–1399. https://doi.org/10.1111/j.1558-5646.2008.00380.x PMID: 18363863

48. Débarre F, Lenormand T, Gandon S. Evolutionary epidemiology of drug-resistance in space. PLoS Computational Biology. 2009; 5(4):e1000337. https://doi.org/10.1371/journal.pcbi.1000337 PMID: 19343211

49. Chabas H, Lion S, Nicot A, Meaden S, van Houte S, Moineau S, et al. Evolutionary emergence of infectious diseases in heterogeneous host populations. PLoS biology. 2018; 16(9):e2006738. https://doi.org/10.1371/journal.pbio.2006738 PMID: 30248089

50. Organization WH, et al. Antimicrobial resistance surveillance in Europe 2022–2020 data. World Health Organization. Regional Office for Europe; 2022.

51. Galvin S, Bergin N, Hennessy R, Hanahoe B, Murphy AW, Cormican M, et al. Exploratory spatial mapping of the occurrence of antimicrobial resistance in E. coli in the community. Antibiotics. 2013; 2 (3):328–338. https://doi.org/10.3390/antibiotics2030328 PMID: 27029306

52. Fu F, Nowak MA, Bonhoeffer S. Spatial heterogeneity in drug concentrations can facilitate the emergence of resistance to cancer therapy. PLoS Comput Biol. 2015; 11(3):e1004142. https://doi.org/10.1371/journal.pcbi.1004142 PMID: 25789469

53. Greulich P, Waclaw B, Allen RJ. Mutational pathway determines whether drug gradients accelerate evolution of drug-resistant cells. Physical review letters. 2012; 109(8):088101. https://doi.org/10.1103/PhysRevLett.109.088101 PMID: 23002776

54. Hermsen R, Deris JB, Hwa T. On the rapidity of antibiotic resistance evolution facilitated by a concentration gradient. Proceedings of the National Academy of Sciences. 2012; 109(27):10775–10780. https://doi.org/10.1073/pnas.1117716109 PMID: 22711808

55. Kepler TB, Perelson AS. Drug concentration heterogeneity facilitates the evolution of drug resistance. Proceedings of the National Academy of Sciences. 1998; 95(20):11514–11519. https://doi.org/10.1073/pnas.95.20.11514

56. Moreno-Gamez S, Hill AL, Rosenbloom DI, Petrov DA, Nowak MA, Pennings PS. Imperfect drug penetration leads to spatial monotherapy and rapid evolution of multidrug resistance. Proceedings of the National Academy of Sciences. 2015; 112(22):E2874–E2883. https://doi.org/10.1073/pnas.1424184112

57. Zhang Q, Lambert G, Liao D, Kim H, Robin K, Tung Ck, et al. Acceleration of emergence of bacterial antibiotic resistance in connected microenvironments. Science. 2011; 333(6050):1764–1767. https://doi.org/10.1126/science.1208747 PMID: 21940899

58. Hermsen R, Hwa T. Sources and sinks: a stochastic model of evolution in heterogeneous environments. Physical review letters. 2010; 105(24):248104. https://doi.org/10.1103/PhysRevLett.105.248104 PMID: 21231560

59. De Jong MG, Wood KB. Tuning Spatial Profiles of Selection Pressure to Modulate the Evolution of Drug Resistance. Phys Rev Lett. 2018; 120:238102. https://doi.org/10.1103/PhysRevLett.120.238102 PMID: 29932692

60. De Jong MG, Wood KB. Tuning spatial profiles of selection pressure to modulate the evolution of drug resistance. Physical review letters. 2018; 120(23):238102. https://doi.org/10.1103/PhysRevLett.120.238102 PMID: 29932692

61. Goossens H, Ferech M, Vander Stichele R, Elseviers M. Outpatient antibiotic use in Europe and association with resistance: a cross-national database study. The Lancet. 2005; 365(9459):579–587. https://doi.org/10.1016/S0140-6736(05)17907-0

62. Asaduzzaman M, Rousham E, Unicomb L, Islam MR, Amin MB, Rahman M, et al. Spatiotemporal distribution of antimicrobial resistant organisms in different water environments in urban and rural settings of Bangladesh. Science of the Total Environment. 2022; 831:154890. https://doi.org/10.1016/j.scitotenv.2022.154890 PMID: 35364179

63. Loewe S. The problem of synergism and antagonism of combined drugs. Arzneimittel-Forschung. 1953; 3(6):285–290. PMID: 13081480

64. Greco WR, Bravo G, Parsons JC. The search for synergy: a critical review from a response surface perspective. Pharmacological reviews. 1995; 47(2):331–385. PMID: 7568331

65. Chait R, Craney A, Kishony R. Antibiotic interactions that select against resistance. Nature. 2007; 446 (7136):668. https://doi.org/10.1038/nature05685 PMID: 17410176

66. Michel JB, Yeh PJ, Chait R, Moellering RC, Kishony R. Drug interactions modulate the potential for evolution of resistance. Proceedings of the National Academy of Sciences. 2008; 105(39):14918–14923. https://doi.org/10.1073/pnas.0800944105

67. Hegreness M, Shoresh N, Damian D, Hartl D, Kishony R. Accelerated evolution of resistance in multidrug environments. Proceedings of the National Academy of Sciences. 2008; 105(37):13977–13981. https://doi.org/10.1073/pnas.0805965105 PMID: 18779569

68. Pena-Miller R, Laehnemann D, Jansen G, Fuentes-Hernandez A, Rosenstiel P, Schulenburg H, et al. When the most potent combination of antibiotics selects for the greatest bacterial load: the smile-frown transition. PLoS biology. 2013; 11(4):e1001540. https://doi.org/10.1371/journal.pbio.1001540 PMID: 23630452

69. Dean Z, Maltas J, Wood KB. Antibiotic interactions shape short-term evolution of resistance in E. faecalis. PLoS pathogens. 2020; 16(3):e1008278. https://doi.org/10.1371/journal.ppat.1008278 PMID: 32119717

70. Gjini E, Wood KB. Price equation captures the role of drug interactions and collateral effects in the evolution of multidrug resistance. eLife. 2021; 10. https://doi.org/10.7554/eLife.64851 PMID: 34289932

71. Barbosa C, Beardmore R, Schulenburg H, Jansen G. Antibiotic combination efficacy (ACE) networks for a Pseudomonas aeruginosa model. PLoS biology. 2018; 16(4):e2004356. https://doi.org/10.1371/journal.pbio.2004356 PMID: 29708964

72. Rodriguez de Evgrafov M, Gumpert H, Munck C, Thomsen TT, Sommer MO. Collateral resistance and sensitivity modulate evolution of high-level resistance to drug combination treatment in Staphylococcus aureus. Molecular biology and evolution. 2015; 32(5):1175–1185. https://doi.org/10.1093/molbev/msv006 PMID: 25618457

73. Munck C, Gumpert HK, Wallin AIN, Wang HH, Sommer MO. Prediction of resistance development against drug combinations by collateral responses to component drugs. Science translational medicine. 2014; 6(262):262ra156–262ra156. https://doi.org/10.1126/scitranslmed.3009940 PMID: 25391482

74. Maltas J, Wood KB. Pervasive and diverse collateral sensitivity profiles inform optimal strategies to limit antibiotic resistance. PLoS biology. 2019; 17(10):e3000515. https://doi.org/10.1371/journal.pbio.3000515 PMID: 31652256

75. Maltas J, Krasnick B, Wood KB. Using selection by nonantibiotic stressors to sensitize bacteria to antibiotics. Molecular biology and evolution. 2020; 37(5):1394–1406. https://doi.org/10.1093/molbev/msz303 PMID: 31851309

76. Roemhild R, Linkevicius M, Andersson DI. Molecular mechanisms of collateral sensitivity to the antibiotic nitrofurantoin. PLOS Biology. 2020; 18(1):1–20. https://doi.org/10.1371/journal.pbio.3000612

77. Ardell SM, Kryazhimskiy S. The population genetics of collateral resistance and sensitivity. eLife. 2021; 10:e73250. https://doi.org/10.7554/eLife.73250 PMID: 34889185

78. Hofbauer J, Sigmund K. Evolutionary games and population dynamics. Cambridge university press; 1998.

79. Maltas J, Killarney ST, Singleton KR, Strobl MA, Washart R, Wood KC, et al. Drug dependence in cancer is exploitable by optimally constructed treatment holidays. Nature Ecology & Evolution. 2024; 8 (1):147–162. https://doi.org/10.1038/s41559-023-02255-x

80. Fisher RA. The wave of advance of advantageous genes. Annals of Eugenics. 1937; 7(4):355–369. https://doi.org/10.1111/j.1469-1809.1937.tb02153.x

81. Kolmogorov AN, Petrovsky IG, Piskunov NS. Investigation of the Equation of Diffusion Combined with Increasing of the Substance and Its Application to a Biology Problem. Bulletin of Moscow State University Series A: Mathematics and Mechanics. 1937; 7(4):1–25.

82. Price GR. Selection and Covariance. Nature. 1970; 227(5257):520–521. https://doi.org/10.1038/227520a0 PMID: 5428476

83. Price GR. Extension of covariance selection mathematics. Annals of Human Genetics. 1972; 35 (4):485–490. https://doi.org/10.1111/j.1469-1809.1957.tb01874.x PMID: 5073694

84. Skellam JG. Random Dispersal in Theoretical Populations. Biometrika. 1951; 38(1-2):196–218. https://doi.org/10.2307/2332328 PMID: 14848123

85. Cantrell RS, Cosner C. The effects of spatial heterogeneity in population dynamics. Journal of Mathematical Biology. 1991; 29(4):315–338. https://doi.org/10.1007/BF00167155

86. Seno H. Effect of a singular patch on population persistence in a multi-patch system. Ecological modelling. 1988; 43(3-4):271–286. https://doi.org/10.1016/0304-3800(88)90008-7

87. Wood KB, Wood KC, Nishida S, Cluzel P. Uncovering scaling laws to infer multidrug response of resistant microbes and cancer cells. Cell reports. 2014; 6(6):1073–1084. https://doi.org/10.1016/j.celrep.2014.02.007 PMID: 24613352

88. Gude S, Pinçe E, Taute KM, Seinen AB, Shimizu TS, Tans SJ. Bacterial coexistence driven by motility and spatial competition. Nature. 2020; 578(7796):588–592. https://doi.org/10.1038/s41586-020-2033-2 PMID: 32076271

89. Berestycki H, Hamel F, Roques L. Analysis of the periodically fragmented environment model I: Species persistence. Journal of Mathematical Biology. 2005; 51(1):75–113. https://doi.org/10.1007/s00285-004-0313-3 PMID: 15868203

90. Berestycki H, Hamel F, Roques L. Analysis of the periodically fragmented environment model II: biological invasions and pulsating traveling fronts. Journal de Mathamatiques Pures et Appliques. 2005; 84(8):1101–1146. https://doi.org/10.1016/j.matpur.2004.10.006

91. Pellacci B, Verzini G. Best dispersal strategies in spatially heterogeneous environments: optimization of the principal eigenvalue for indefinite fractional Neumann problems. Journal of Mathematical Biology. 2018; 76(6):1357–1386. https://doi.org/10.1007/s00285-017-1180-z PMID: 28889217

92. Aronson DG, Weinberger HF. Multidimensional nonlinear diffusion arising in population genetics. Advances in Mathematics. 1978; 30(1):33–76. https://doi.org/10.1016/0001-8708(78)90130-5

93. Kinezaki N, Kawasaki K, Takasu F, Shigesada N. Modeling biological invasions into periodically fragmented environments. Theoretical population biology. 2003; 64(3):291–302. https://doi.org/10.1016/S0040-5809(03)00091-1 PMID: 14522170

94. Shigesada N, Kawasaki K, Teramoto E. Traveling periodic waves in heterogeneous environments. Theoretical Population Biology. 1986; 30(1):143–160. https://doi.org/10.1016/0040-5809(86)90029-8

95. Griette Q, Alfaro M, Raoul G, Gandon S. Evolution and spread of multidrug resistant pathogens in a spatially heterogeneous environment. bioRxiv. 2022;p. 2022–07.

96. Cantrell RS, Cosner C. Diffusive logistic equations with indefinite weights: population models in disrupted environments. Proceedings of the Royal Society of Edinburgh Section A: Mathematics. 1989; 112(3-4):293–318. https://doi.org/10.1017/S030821050001876X

97. Young E, Allen RJ. Lineage dynamics in growing biofilms: Spatial patterns of standing vs. de novo diversity. Frontiers in microbiology. 2022; 13. https://doi.org/10.3389/fmicb.2022.915095 PMID: 35966660

98. Sinclair P, Carballo-Pacheco M, Allen RJ. Growth-dependent drug susceptibility can prevent or enhance spatial expansion of a bacterial population. Physical Biology. 2019; 16(4):046001. https://doi.org/10.1088/1478-3975/ab131e PMID: 30909169

99. Larsson DJ, Flach CF. Antibiotic resistance in the environment. Nature Reviews Microbiology. 2022; 20(5):257–269. https://doi.org/10.1038/s41579-021-00649-x PMID: 34737424

100. Malagón-Rojas JN, Barrera ELP, Lagos L. From environment to clinic: the role of pesticides in antimicrobial resistance. Revista Panamericana de Salud Pública. 2020; 44. https://doi.org/10.26633/RPSP.2020.44 PMID: 32973897

101. Jiang L, Bao A, Guo H, Ndayisaba F, et al. Vegetation dynamics and responses to climate change and human activities in Central Asia. Science of the Total Environment. 2017; 599:967–980. https://doi.org/10.1016/j.scitotenv.2017.05.012 PMID: 28505889

102. Wicaksono WA, Egamberdieva D, Berg C, Mora M, Kusstatscher P, Cernava T, et al. Function-based rhizosphere assembly along a gradient of desiccation in the former Aral Sea. Msystems. 2022; 7(6):e00739–22. https://doi.org/10.1128/msystems.00739-22 PMID: 36377901

103. Maciel GA, Lutscher F. Movement behaviour determines competitive outcome and spread rates in strongly heterogeneous landscapes. Theoretical Ecology. 2018; 11:351–365. https://doi.org/10.1007/s12080-018-0371-6

104. Estrela S, Brown SP. Community interactions and spatial structure shape selection on antibiotic resistant lineages. PLoS computational biology. 2018; 14(6):e1006179. https://doi.org/10.1371/journal.pcbi.1006179 PMID: 29927925

105. Yurk BP, Cobbold CA. Homogenization techniques for population dynamics in strongly heterogeneous landscapes. Journal of biological dynamics. 2018; 12(1):171–193. https://doi.org/10.1080/17513758.2017.1410238 PMID: 29228877

106. Metz JA, Nisbet RM, Geritz SA. How should we define 'fitness' for general ecological scenarios? Trends in ecology & evolution. 1992; 7(6):198–202. PMID: 21236007

107. Ghosh OM, Good BH. Emergent evolutionary forces in spatial models of luminal growth and their application to the human gut microbiota. Proceedings of the National Academy of Sciences. 2022; 119(28):e2114931119. https://doi.org/10.1073/pnas.2114931119

108. Cremer J, Segota I, Yang Cy, Arnoldini M, Sauls JT, Zhang Z, et al. Effect of flow and peristaltic mixing on bacterial growth in a gut-like channel. Proceedings of the National Academy of Sciences. 2016; 113(41):11414–11419. https://doi.org/10.1073/pnas.1601306113

109. Cremer J, Arnoldini M, Hwa T. Effect of water flow and chemical environment on microbiota growth and composition in the human colon. Proceedings of the National Academy of Sciences. 2017; 114(25):6438–6443. https://doi.org/10.1073/pnas.1619598114 PMID: 28588144

110. Labavić D, Loverdo C, Bitbol AF. Hydrodynamic flow and concentration gradients in the gut enhance neutral bacterial diversity. Proceedings of the National Academy of Sciences. 2022; 119(1):e2108671119. https://doi.org/10.1073/pnas.2108671119 PMID: 34969835

111. Le TMT, Gjini E, Madec S. Quasi-neutral dynamics in a coinfection system with N strains and asymmetries along multiple traits. Journal of Mathematical Biology. 2023; 87(3):48. https://doi.org/10.1007/s00285-023-01977-7 PMID: 37640832

112. Le TMT, Madec S. Spatiotemporal evolution of coinfection dynamics: a reaction–diffusion model. Journal of Dynamics and Differential Equations. 2023;p. 1–46. https://doi.org/10.1016/j.jde.2023.08.032

113. Raymond B. Five rules for resistance management in the antibiotic apocalypse, a road map for integrated microbial management. Evolutionary applications. 2019; 12(6):1079–1091. https://doi.org/10.1111/eva.12808 PMID: 31297143